CALIFORNIA
ENERGY COMMISSION

Energy Research and Development Division

FINAL PROJECT REPORT

Indirect Gas-Fired Dryer with Thermal Driven Ejector System for Bulk Food Processing

Development and Demonstration in California

Gavin Newsom, Governor
March 2020 | CEC-500-2020-018

PREPARED BY:

Primary Authors:
Yaroslav Chudnovsky
Olexiy Buyadgie
Dmytro Buyadgie
Erin Case

1700 S Mount Prospect Road
Des Plaines, Il 60018
Phone: 847-768-0500 | Fax: 847-768-0501
http://www.gti.energy

Contract Number: PIR-14-001

PREPARED FOR:
California Energy Commission

Michael Lozano, P.E.
Project Manager

Virginia Lew
Office Manager
ENERGY EFFICIENCY RESEARCH OFFICE

Laurie ten Hope
Deputy Director
ENERGY RESEARCH AND DEVELOPMENT DIVISION

Drew Bohan
Executive Director

ACKNOWLEDGEMENTS

The authors acknowledge the California Energy Commission, Southern California Gas Company, and the members of Utilization Technology Development, NFP for their financial support of this challenging effort.

The authors are also grateful to Tetra Tech, Inc. and Almega Environmental for providing outstanding measurement and verification services to the project, including independent measurements and South Coast Air Quality Management District compliance testing.

The project demonstration was hosted by Martin Feed, LLC, a family-owned and operated cattle feed business in operation since the 1960s. Martin Feed processes the entire range of collected bakery products such as bread, dough, crackers, pastries, pies, tortillas, and cookies.

PREFACE

The California Energy Commission's Energy Research and Development Division manages the Natural Gas Research and Development program, which supports energy-related research, development, and demonstration not adequately provided by competitive and regulated markets. These natural gas research investments spur innovation in energy efficiency, renewable energy and advanced clean generation, energy-related environmental protection, energy transmission and distribution, and transportation.

The Energy Research and Development Division conducts this public interest natural gas-related energy research by partnering with RD&D entities, including individuals, businesses, utilities, and public and private research institutions. This program promotes greater natural gas reliability and lower costs, increases safety for Californians, and is focused in these areas:

- Buildings End-Use Energy Efficiency
- Industrial, Agricultural, and Water Efficiency
- Renewable Energy and Advanced Generation
- Natural Gas Infrastructure Safety and Integrity
- Energy-Related Environmental Research
- Natural Gas-Related Transportation

Indirect Gas-Fired Dryer with Thermal Driven Ejector System for Bulk Food Processing is the final report for the Thermo-vacuum Ejector-Based Drying System Demonstration in California project (Contract Number PIR-14-001) conducted by Gas Technology Institute. The information from this project contributes to the Energy Research and Development Division's Natural Gas Research and Development Program.

For more information about the Energy Research and Development Division, please visit the Energy Commission's research website (www.energy.ca.gov/research/) or contact the Energy Commission at 916-327-1551.

ABSTRACT

The drying of materials – whether solids, liquids, or slurries – to improve storage life, meet technological requirements, or reduce transportation costs is one of the oldest and most common industrial processing operations. Drying is an energy-intensive operation often consuming more than 50—60 percent of total energy input required for the entire process. In California, dried and dehydrated fruits and vegetables processing are estimated to consume more than 6.2 trillion Btu of energy per year. Improving the energy efficiency of industrial drying equipment will yield significant energy savings and greenhouse gas reduction across the diversified industrial market. This project demonstrated a natural gas-fired drying technology that provides cost and environmental benefits for a broad range of agricultural and industrial applications. The concept involves integrating a drying process with an innovative thermal driven ejector system. The full-scale demonstration of this concept at a California food processor was successful to prove the effectiveness of the ejector system in producing adequate dynamic vacuum and acting as an integrated heat pump. However, mechanical challenges with the system provide an opportunity for further development and demonstration of the thermo-vacuum drying system as the next step in commercializing this energy-efficient alternative to traditional drying technologies.

Keywords: Low NO_X combustion system, ejector, holo-flite, heat pump, bulk food product, drying

Please use the following citation for this report:

Yaroslav Chudnovsky et al. Gas Technology Institute. 2020. Indirect Gas-Fired Dryer with Thermal Driven Ejector System for Bulk Food Processing: Development and Demonstration in California. California Energy Commission. Publication Number: CEC-500-2020-018.

TABLE OF CONTENTS

LIST OF FIGURES

Page

LIST OF TABLES

Page

EXECUTIVE SUMMARY

Introduction

The drying of materials – whether solids, liquids, or slurries – to improve storage life, meet technological requirements, or reduce transportation costs is one of the oldest and most commonly used operations. Drying is an energy-intensive operation often consuming more than 50 percent to 60 percent of total energy input required for the entire process. In many cases, drying is the most energy-intensive and temperature-critical aspect of food, chemical, and pharmaceutical product processing. Improving the energy efficiency performance of industrial drying equipment will have a highly beneficial effect on energy conservation and greenhouse gas reduction in numerous food and chemical industries.

Project Purpose

This project designed and demonstrated in a commercial setting an emerging technology for industrial food and agricultural drying applications. This technology aims to save energy, improve drying operation efficiency, and improve heat and water recovery using an innovative heat pump design. A heat pump is a device that transfers heat energy from a source of heat to a heat sink. Heat pumps move thermal energy by absorbing heat from a cold space and releasing it to a warmer one. This technological approach could be applied for drying or thermal processing of bulk solids across a wide spectrum of industrial and commercial applications (chemical granules, biomass pellets, pharmaceutical products, etc.). Successful demonstration of the technology and its cost and environmental benefits will speed its introduction to the industrial, agriculture, and water sectors in California.

Gas Technology Institute (GTI) with its industrial partners, designed, engineered, fabricated, installed, monitored, and evaluated a gas-fired thermo-vacuum dryer at a California industrial food-processing site, Martin Feed, LLC (www.martinfeedllc.com). Martin Feed, LLC produces cattle feed for dairy farms throughout California.

Ejectors belong to the jet compression apparatus class. These devices have no moving parts and use the potential energy generated by the burners to create useful kinetic energy. Two major functions of ejectors are as compressors, in which they are used to compress gases, or as producers of a vacuum. In this project the ejectors are used for both purposes: they create a vacuum in the rotary dryer chamber, and they are also used to recompress the evaporated moisture from the product to recover heat from the moisture.

Project Process

The major steps in this project included:

- Detailed drying system specification, analysis, and design per host site application requirements, taking into account the existing operating performance and required product quality.
- Field engineering, fabrication, and procurement of the major system components, including controls, measurement, and data acquisition systems with a potential for further integration with the plant control panel.
- Installation, shakedown, data collection, and processing at the host site facility.
- Results analysis, final reporting, and recommendations for the commercial system, along with technology and knowledge transfer activities.

Project Results

Industrial drying is characterized by the effectiveness and efficiency of the length of drying time, energy consumption, capital and operating costs, as well as product quality and environmental compliance. This successful commercial-scale demonstration of the thermo-vacuum process used in this technology significantly improved the drying time and energy consumption of the system, while reducing environmental impact.

To reduce product moisture content from 35 percent to 12 percent, the drying system must remove 84 pounds of moisture per minute. A standard drying process would use 5.4 million British thermal units per hour (MMBtu/hr) to heat the materials and an additional 10-15 MMBtu/hr to heat air circulated through the system to remove the moisture evaporated from the materials. This new drying system technology requires only 6.7 MMBtu/hr to provide the heating and vacuum that delivers the airflow to remove the moisture evaporated from the materials. This results in natural gas savings of 61-65 percent or about 12-13 MMBtu/hr for the same drying product throughput. Assuming 500,000 tons per year of dried products market in California, the annual natural gas savings would represent 2-2.5 billion cubic feet of gas or $12-$15 million (assuming gas price of $6/MMBtu) and about 4-4.5 megawatt hours of saved electricity and 80 million gallons of recovered water.

Taking into account the adequate replacement of recirculation pumps and air fans for the ejectors and heat exchangers, capital costs could be reduced by 50 percent or more.

The project demonstrated the designed performance of the ejector system for product throughput of 366 pounds of wet material per minute (around 11 tons per hour). The ejectors evacuated about 85.9 pounds per minute of air-moisture where the air mass portion was less than 1.5 percent. However, taking into account minor leakages in the sealed chambers, the nominal moisture evacuation rate by ejectors should be 47.5 pounds per minute to provide the dried product moisture content at the designed level of 12 percent to 15 percent. The need to optimize parameters of the drying process by considering differences in product type, throughput variations, and vacuum dynamics should be the subject of follow-on efforts.

Benefits to California

The successful implementation of gas-fired thermo-vacuum dryer technology with advanced heat pump system integration in industrial food processing offers significant energy savings for California. The technology concept can be also adapted to other drying and food processing applications besides the screw-type dryer specifically used in this demonstration. Application will result in end-user fuel savings (more than 60 percent), reduced pollutant emissions (at least 10 percent), and the strong potential for moisture recovery and reuse.

Integrating heat pumps into the thermovacuum drying system greatly enhances its performance efficiency, economics, and greenhouse gas emissions reductions. The research team estimates that an electric heat pump with an assumed coefficient of performance of 6 and an ejector-based heat pump with a projected coefficient of performance of 2 could provide cost savings of 6 percent and 63 percent, respectively, when compared to direct-fired gas drying.

The expected environmental benefits are significant. The higher efficiency of the integrated thermovacuum system compared to traditional rotary dryers means the user consumes less fuel, which means fewer combustion emissions including carbon dioxide and other pollutants. Further environmental benefits could be captured though moisture recovery from the system exhaust, which users could apply as complementary hot water services or irrigation.

The indirect gas-fired drying market accounts for about 5 percent of the total natural gas consumption across the United States commercial and industrial sectors. According to the Energy Information Administration, commercial and industrial customers nationwide consumed about 10 trillion cubic feet of natural gas in 2012, and indirect drying operations consumed about 0.5 trillion cubic feet. Applying the thermovacuum technology (with at least 75 percent energy efficiency) to 100 percent of the commercial and industrial gas-fired drying processes would provide energy savings of about 60 percent, or about 0.3 trillion cubic feet per year, compared to conventional operations. Considering market growth over the last decade, and assuming a natural gas price of at least $5/MMBtu, the demonstrated thermovacuum drying technology has the potential to save more than 200 tons of CO_2 per year in California for agricultural drying operations.

CHAPTER 1:
Introduction and Importance

The drying of materials – whether solids, liquids, or slurries – to improve storage life, meet technological requirements, or reduce transportation costs is one of the oldest and most commonly used operations. Drying is an energy-intensive operation often consuming over 50—60 percent of total energy input required for the entire process. In many cases, drying is the most energy-intensive and temperature-critical aspect of food, chemical, and pharmaceutical product processing. Improving the energy efficiency performance of industrial drying equipment will have a highly beneficial effect on energy conservation and greenhouse gas (GHG) reduction in numerous food and chemical industries.

1.1 Current State of Bulk Food Product Drying Technology

Agricultural drying process operators currently rely on traditional low-efficiency tunnel dryers, gas-fired rotary dryers, or fluid bed dryers. Many products require custom design of dryers to ensure that particle integrity and drying specifications are met. In addition to agricultural applications, these drying technologies are used in a variety of other industrial processes such as food processing, pharmaceuticals, chemicals, mining, and textiles. Some operators rely on open-air sun-drying processes; however, this is a much slower and less controlled process and yield is affected by the weather. Drying under controlled conditions is more common and ensures consistency in quality, while also speeding up the drying process.

Many dryers are convective, or direct-heated, dryers, which use the sensible heat of a gas in contact with wet solids to vaporize moisture and remove it from the chamber. In agricultural applications, the moisture is water, and the water is removed to the atmosphere. It is impractical to try and recover this moisture considering the large volume of gas it is contained in. Significant energy is lost through the exhaust gas.[1] Direct-fired heating is limited by food safety requirements due to the requirement to avoid direct contact between the combustion product and the processed foods.

Another subset of dryers is contact, or indirect-heated, dryers, in which the heat needed to dry the product is transferred through a wall. This dryer type can be much more expensive to design and fabricate; however, it allows operation under vacuum and provides better energy efficiency since the energy lost through exhaust gas is greatly reduced [1]. The use of heat and vacuum (thermo-vacuum) in drying processes is widely known. It is superior to other processes in terms of the speed of drying and the drying quality. However, driving the vacuum pump is an energy-intensive process.

The traditional drum dryer is an indirect-heated system where the heat is supplied from the inside of a metal cylinder (in most cases by pressurized condensing steam) or by

direct-fired air heating, while the product (such as slurry, powder, paste, etc.) is supplied from the outside to the rotating shell in a thin sheet. The product is then scraped by the doctor blade after being dried to pre-determined moisture conditions during less than one revolution. Various feed systems for drum dryers are shown in Figure 1. The use of steam requires the drums to meet American Society of Mechanical Engineers (ASME) codes for pressure vessels, which limits the steam pressure and, consequently, the shell temperature. This reduces drying capacity.

Figure 1: Drum Dryer Typical Feed Systems

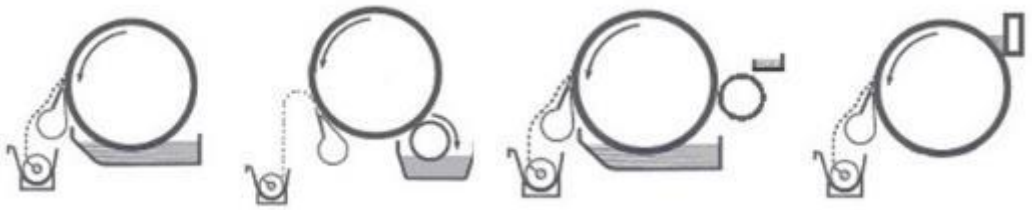

Source: https://simon-dryers.co.uk/en/ma/2/DrumFlaker.html

The conventional gas-fired rotary drum dryers (Figure 2) are metal cylinders heated by condensing steam or by direct-fired air heating. In direct-fired systems, the combustion products flow through the inclined rotating cylinder where the bulk solid material is travelling, moved along and tumbled through the heating gas by internal flights. Indirect-heated systems apply heat to the shell of the drum using a steam jacket, oil heating, or furnace encasement of the rotary drum [2].

Figure 2: Direct Fired Rotary Drum Dryer

Source: Directindustry.com

Fluid bed dryers (Figure 3) convey the product along via a perforated belt within an enclosed vessel. Hot dry air passes up through the belt and the product. In some instances, the vessel also vibrates to enhance fluidization of the product. The mixture of upward directed air and vibration results in a large degree of fluidization and promotes air contact with the product [3].

Figure 3: Fluid Bed Dryer for Bulk Food Processing

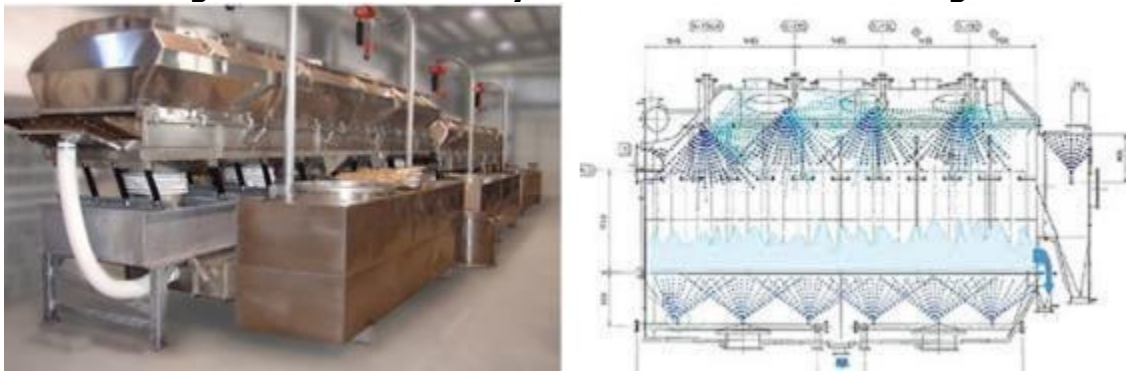

Source: https://www.foodengineeringmag.com/articles/89953-fluid-bed-dryercooler

Screw dryers, similar to rotary drum dryers, are able to process large volumes of product. These large jacket dryers move the product via screws with hollow flites. The jacket and the screws can be heated by steam or another thermal fluid.

Drum drying or drum heating is used in a variety of industrial processes such as pharmaceuticals, chemicals, textiles, etc. Gas-fired rotary dryers are more commonly used in industrial processes involving more heavy-duty materials. Screw dryers are often seen in the mining industry.

Beyond the dryer types described above, bulk food processing may use tunnel dryers, kiln dryers, tray dryers, spray dryers, pneumatic dryers, and freeze dryers, among others.

1.1.1 Motivation

There are two major forces driving the development of improved drying operations in the food processing market: (1) low energy efficiency, and (2) the high cost of state-of-the-art drying technologies and associated equipment. Drying is an energy-intensive operation, often consuming more than 50—60 percent of total energy input required for the entire process of processing, modifying, and transporting a material. In California, it is estimated that dried and dehydrated fruits and vegetables processing consumes more than 6.2 trillion Btu (TBtu) total energy per year [4].

The thermo-vacuum drying process has been known for a many years, but its application has not become widespread. This process consumes a large amount of heat for moisture evaporation, and significant electrical energy to drive the water-ring vacuum pump. If the vacuum is very deep (0.0385-0.0965 pounds per square inch [psi]; 1.1—2.7 inch of water column; 2—5 mmHg), the power consumption can exceed 30 kW per 1 ton (2204.6 lb) of the dried product per hour. At the same time, the drying quality and speed is superior to other drying methods. Therefore, this project looks to implement a progressive method of drying under vacuum while minimizing the consumption of energy, mainly natural gas.

The gas-fired thermal-vacuum drying (GFTD) with integrated heat pump (HP) technology (GFTD-HP) has not been proven in a production environment prior to this project. Demonstrating the GFTD-HP technology's potential to provide energy savings and emission reductions will help clear the path to commercial availability. The large amount of capital already invested in existing drying processes hinders adoption of new high-capital equipment. Although GFTD-HP is expected to be slightly more expensive than current dryers, its adoption potential will be contingent to the level of fuel savings. Increased efficiency of the drying operation, water recovery, and other benefits including anticipated product quality improvement will be demonstrated in this project. These results will provide solid fiscal and market reasons to adopt this new drying technology. Drying equipment will only be adopted when proven to be as reliable as existing dryers. The goal of demonstration testing at the participating feed processor plant in this project was to determine the technology's reliability compared to existing dryers and to understand the difficulty and cost of retraining operators.

New technologies are rarely adopted in static or shrinking industries. Agricultural drying demand has grown over the decades and is expected to continue growing. Therefore, as new demand requires purchase of new dryers, this technology is well-positioned to fill the need as it is further developed. In addition, the cross-cutting nature of this new drying technology will help overcome barriers associated with capital cost and adoption of a new technology.

1.2 Project Description

The purpose of this project was to design and demonstrate in a commercial setting a superior drying technology for bulk food and agricultural drying applications that would save energy, improve drying operation efficiency, and improve heat and water recovery through the use of an innovative heat pump.

1.2.1 Background

Gas Technology Institute (GTI) developed an innovative high-efficiency gas-fired drum dryer (GFDD) concept based on a combination of a ribbon flame and an advanced heat transfer enhancement technique. The concept was successfully proven in full-scale demonstrations of the GFDD for paper drying and food powder toasting, using heat supplied from the inside of the drum while dried product is applied from the outside [CEC-500-2010-043]. The full-scale demonstrations indicated the strong potential for the technology to be used in retrofit and new applications as a cost-effective alternative to steam-heated systems. Figure 4 presents the full-scale dryer and drying rate for the entire range of GTI demonstrations.

Figure 4: Gas Technology Institute Full-Scale Demonstration of Gas-Fired Drum Dryer for the Linerboard Drying and TAPPI Drying Rates

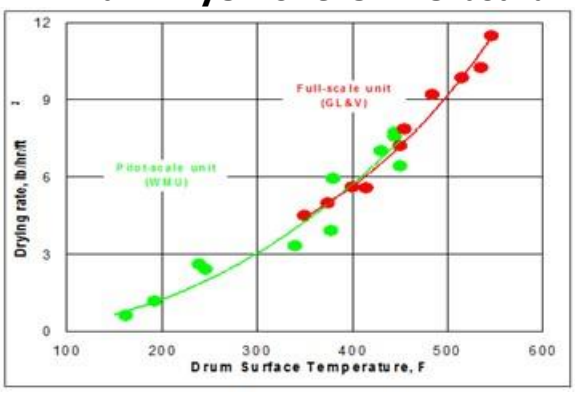

Source: GTI

The original proposed GTI-patented [US 6,877,979] approach of all-in-one indirect gas-fired rotary dryer with heat pump (IGFRD-HP) offered a high-efficient and cost-effective gas-fired technology for the indirect drying and thermal treating of bulk solids such as grains, rice, beans, granular chemicals, pellets, sand, etc. Integrating the drying process with a thermal-vacuum ejector-based system and advanced heat pump, as shown in Figure 5, was anticipated to further improve efficiency and production. The product drying could be realized in a wide range of process temperatures and throughputs, providing reliable operation with enhanced product quality and improved energy efficiency.

Figure 5: General Layout of Gas-Fired Drying Process

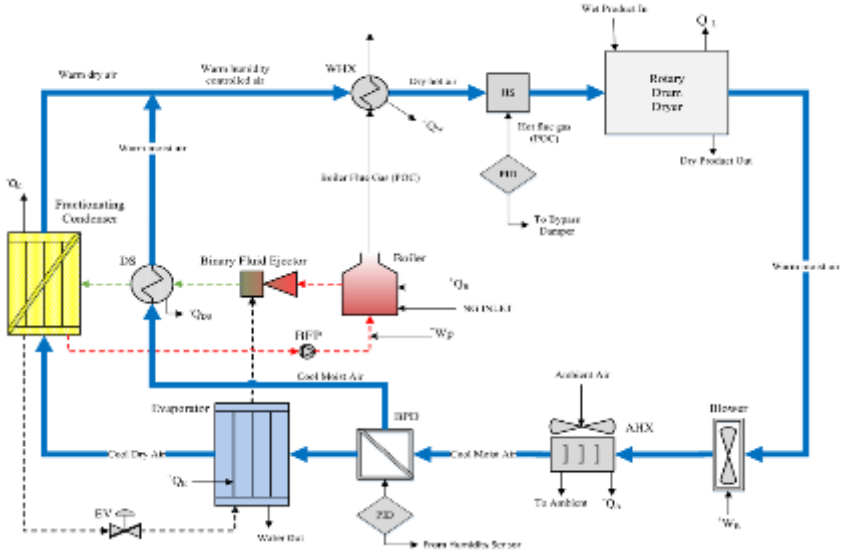

Source: May-Ruben Technologies Inc.

The incorporation of heat pumps into the drying process has, for decades, offered the promise of lower energy use and enhanced operations through better control of dehumidification during the drying process. Unfortunately, it has only been deployed in

a relatively small number of installations, mostly for use in drying lumber. To ensure a favorable environmental impact, the proposed IGFRD-HP was expected to provide the end-user with fuel savings by producing fewer pollutant emissions as opposed to the traditional rotary dryers. Moisture recovery from the IGFRD-HP exhaust would provide additional benefits to end-users in the form of ware washing and hot water services.

When the original host site, Inland Empire Foods, was no longer able to participate in the demonstration, a new host site, Martin Feed, LLC, was identified. The weight of product requiring processing at Martin Feed was significantly higher (~ 100 t/d) than that at Inland Empire Foods (~ 20 t/d), so the technology had to be modified accordingly to handle the higher throughput of feed. The same benefits apply, but the GFTD process with an innovative heat pump technology was instead modified for integration with a rotary screw dryer, rather than a rotary drum dryer. The nature of the product made the rotary screw dryer a good choice for high throughput operations of granular solids.

1.2.2 Objectives

The goal of the Agreement [PIR-14-001] was to demonstrate the performance benefits of an innovative GFTD process integrated with an innovative heat pump technology for highly efficient and environmentally friendly indirect drying of bulk agricultural and food products. The demonstrated approach can also be successfully applied for drying or thermal processing of bulk solids across the wide spectrum of industrial and commercial applications (chemical granules, biomass pellets, pharmaceutical products, petcoke charges, etc.) by providing energy efficient heating and waste heat and water recovery/reuse at a low operating cost and an environmentally friendly impact level. Successful demonstration of the technology will speed the introduction into the California market of improved natural gas-fired drying technologies with cost and environmental benefits through reductions in the use of natural gas in California's industrial, agricultural, and water (IAW) industrial sector.

The performance success metrics for the demonstration included (1) the reliable mechanical operation of the demonstration system, and (2) the quality of the product evaluated at the host site product quality laboratory, using industry-established methods and procedures. The demonstration also met State of California compliance requirements for natural gas combustion, as measured by SCAQMD-certified contractor Almega Environmental.

The stated objectives of this project were to:

- Improve efficiency of bulk foods drying operations to over 75 percent.
- Reduce natural gas consumption for the same throughput by at least 60 percent.
- Reduce primary energy consumption by 10—15 percent.
- Prove the cost-effectiveness of successful integration of the advanced heat pump into drying operations.

- Prove the benefits and facilitate the transformation of the drying market through demonstration.

Testing of the GFTD-HP process at a participating processing facility demonstrated that the technology's feasibility and reliability is similar to existing dryers and that retraining of operators is not difficult or costly.

1.3 Market Impact

There is an ongoing need for new energy-saving technologies for industrial combustion applications. The capabilities of the proposed technology can be successfully transferred to and be of a great deal of benefit for natural gas-fired industrial processes by improving energy efficiency and reducing pollutant emissions while providing energy savings for drying bulk foods. Advanced technologies that reduce energy demand in California always benefit the California ratepayers. Water recovery from the product moisture can provide additional benefits to end-users in the form of livestock, irrigation, or other water services.

The incorporation of heat pumps into the drying process offers the promise of lower energy use and enhanced operations through better control of dehumidification during the drying process. To date, this technology has been deployed in a relatively small number of installations. The advanced heat pump technology was integrated into the demonstration drying system to significantly enhance its performance efficiency, economics, and reduction of greenhouse gas emissions. Integrating the higher-efficiency GFTD and the heat pump provides significant energy savings and carbon dioxide (CO_2) emissions reductions. The GFTD increases the dryer efficiency from the present 25 percent—62 percent to a projected 75 percent and above.

The indirect gas-fired drying market is conservatively estimated to account for about 5 percent of total natural gas consumption across the full range of commercial and industrial sectors. Applying the high efficiency GFTD heat pump technology to commercial and industrial gas-fired drying processes would achieve energy savings of nearly 60 percent, or roughly 288 quads nationwide with 100 percent market penetration.

The combined heat pump and thermo-vacuum rotary dryer technologies presents an opportunity to affect end-user natural gas savings in a number of agricultural and industrial drying applications.

Based on preliminary estimates, the conservative potential for the indirect gas-fired drying market accounts for about 5 percent of total natural gas consumption across the commercial and industrial sectors nationwide. Per the United States Energy Information Administration (USEIA), about 11 trillion cubic feet (TCF) of natural gas was consumed in 2017 by commercial and industrial customers nationwide, and indirect drying operators consumed about 0.6 TCF. At the average energy efficiency of the typical dryers – approximately 35—40 percent – the wasted energy from these drying

processes can be estimated at 3,500 million therms. Applying GFTD-HP technology with at least 75 percent energy efficiency to commercial and industrial gas-fired drying processes achieves energy savings of approximately 60 percent compared to conventional operations.

The successful demonstration of this unique and challenging technology in a full-scale production environment could create strong interest from the California-based industrial food processors in replacing the inefficient and, in most cases, costly drying installations with a cost-effective and environmentally friendly alternative. The efficiency improvement and water/heat recovery/reuse option will preserve natural resources for California and will reduce natural gas consumption by California natural gas ratepayers, along with decreasing carbon monoxide (CO), nitrogen oxides (NO_X) and CO_2 emissions.

Agricultural drying demand is expected to continue to grow. As new demand requires the purchase of new dryers, this technology is well-positioned to fill the need. This project brings to the marketplace an advanced high-efficiency drying technology that integrates a gas-fired thermal-vacuum drying process with an innovative heat pump technology.

Considering the state's dried food production capacity spread over a population of about 40 million people, the energy consumption for drying purposes can be three times lower that is equal to save of at least 10 TBtu of heat and contributes to water conservation and other environmental improvements in California.

CHAPTER 2:
Gas-Fired Thermal Vacuum Drying Technology: Description and Design

The demonstrated technology combines a traditional rotary dryer with a thermal driven ejector system and heat pump. The all-in-one indirect gas-fired drying system integrated with a thermal driven ejector system (TDES) offers a highly efficient and cost-effective alternative to the state-of-the-art technologies for the indirect drying and thermal processing of bulk solids, with the option of temperature profiling as well as waste heat and water recovery and reuse.

Controlled heat-input to the product is provided while a vacuum is pulled through the use of ejectors. The combination of heat and vacuum allows the product to be dried to specified moisture requirements in a shorter time. The system was designed by Wilson Engineering Technologies, an engineering company with over 40-years of experience in ejector technologies and heat pumps, focusing on thermal driven ejector systems and heat pump technology development and commercialization. Clayton Boiler, a major boiler manufacturer, supplied their commercially available low-emission steam generation system and controls.

Product drying can be achieved using a wide range of process temperatures and throughputs, providing reliable operation with enhanced product quality and improved energy efficiency. Employing commercially available off-the-shelf low NOx combustion systems provides the opportunity to reduce combustion emissions in industrial and commercial drying operations.

2.1 Thermal Driven Ejector System

Ejectors belong to the jet compression apparatus class. The working or driving force for compression is the potential energy of a fluid medium under the action of the highest pressure in the cycle; potential mechanical energy of pressure can be converted into kinetic energy in the process of flow through profiled holes. The energy thus obtained is partially transferred to the low-pressure passive stream, which is subsequently converted into potential pressure energy, and thereby compressed.

The fact that TDES uses no moving parts means that in its design conditions it is extremely reliable and low maintenance, with no source of power necessary besides the motive gas. Thermal driven ejector systems produce a low level of sound emission.

Jet devices are distinguished by their versatility. They are used as jet compressors (i.e., ejectors), as jet pumps or injectors, as elevators, as jet heaters, as vacuum pumps, and, finally, as heat pumps. Recently, another function of ejectors has emerged – these are jet exhaust fans. Ejectors can be used in various fields, including but not limited to

refrigeration, cryogenic and heat engineering, the construction industry, thermal power plants, food processing, and chemical and transport industries.

Two major functions of ejectors are as fluidic compressors, in which they are used to compress low pressure gases, or as producers of a dyn vacuum. In the current application, the ejectors are used for both purposes: they create a dynamic vacuum in the rotary dryer chamber, and they are also used to recompress the evaporated moisture from the product as a component in the heat pump system to recover heat from the evaporated moisture from the product.

A steam jet ejector is an alternative to a mechanical vacuum pump or to a mechanical compressor in a heat pump cycle. In both cases, the ejector uses heat and does not require electricity for work. In their application for refrigeration or heat pump cycles, the advantages of a jet heat pump compared to a traditional compressor are as follows:

- The thermal power station, electric power transmission line and compressor are replaced, essentially, with just a pipe section with channels of a given shape and size.
- The average potential heat used for the jet heat pump operation is 150—200°C, which is in the range of combustion products or concentrated solar temperatures.
- There are not any energy losses associated with electricity transmission over long distances and voltage transformation.
- Ejectors can work at relatively high temperatures, which is necessary for cycles similar to the process at Martin Feed. A conventional compressor heat pump in these modes is generally inoperative, having a temperature limit of 60—80°C.

The advanced drying system was enhanced with a thermal sub-atmospheric technique that was integrated with the advanced heat pump scheme to significantly improve the performance of the drying operation. In application to thermo-vacuum drying of food products, the ejectors are used both to pull a vacuum on the rotary dryer vessel and to collect and recover the low-quality water vapor that is coming from the product. Ejectors use the motive steam for vacuum production at the expense of natural gas combustion. This high-pressure steam evacuates the heat of evaporation along with the evaporated moisture from the drying product. This heat is two-fold higher than the steam generation heat.

Figure 6 shows a schematic of the ejectors on top of the dryer jacket. Additional ejector layout diagrams are shown in Appendix A.

Figure 6: Ejectors, Side View

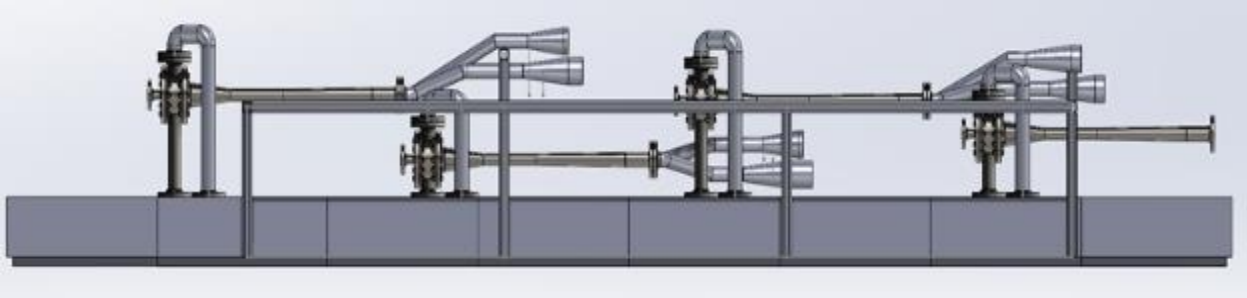

Source: Wilson Engineering

2.1.1 Ejector Operating Principle

The basic operation of an ejector is based on the use of a fluid as the motive force. The motive or working fluid (in this case, high pressure, low velocity saturated or superheated steam) enters through an expanding nozzle, reaching transonic or supersonic speed. The controlled expansion of the steam converts the pressure energy to velocity, creating a vacuum and drawing the suction fluid (in this case, the evaporated moisture from the product) into the mixing chamber from the low-pressure zone. The high velocity motive fluid entrains and mixes with the suction fluid and transmits to it a part of its kinetic energy through direct contact by collision of the flows. The mixed fluid passes through the convergent throat and divergent portions of the Venturi nozzle, accompanied by nearly reversible conversion of kinetic energy into potential energy of pressure due to the smooth increase in the cross section. Thus, at the outlet of the ejector diffuser we obtain a hindered flow at a given intermediate pressure. In this case, the ejector simultaneously performs the function of a vacuum pump, a compressor, and a heat pump. A schematic drawing of an ejector flow part is shown in Figure 7 and more detailed descriptions of the principles of ejector operation and design are found in Appendix B..

Figure 7: Schematic Diagram of an Ejector

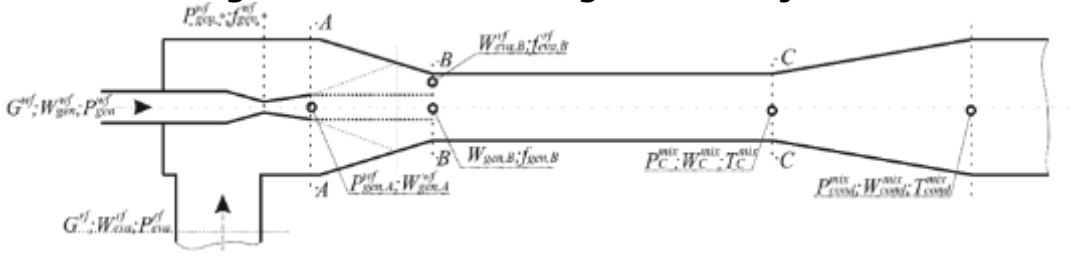

(A) Nozzle outlet cross-sectional area, (B) cylindrical mixing chamber inlet cross-sectional area and (C) cylindrical mixing chamber outlet cross-sectional area.

Source: Gas Technology Institute

2.2 Thermo-Vacuum Process

Known thermal vacuum processes have a separate node for heating the medium from which moisture is being removed and a separate node that creates a vacuum. Thermo-

vacuum processes based on ejector technologies combine not only these two functions, but also produce heat transfer from a lower temperature level to a higher one. In this sense, this process corresponds to the process in the heat pump. In the suction space, a binary mixture of water vapor and air is pumped out along with the heat that is transferred to the dried product from the heating surface. This heat enters the heater after the same ejector. Thus, the heat expended on the production of working steam in the ejector transfers heat from the dried product to a higher temperature level, i.e., performs a heat pump cycle operating on a binary mixture of air and water vapor. Since the ejection coefficient, which is the ratio of the mass flow rate of the vapor-air mixture to the working steam consumption from the steam generator, is about equal to 1 in the cycle, after half of the vapor-air mixture has returned to heating the product, the same amount of heat remains that can be used for other purposes. The cycle also produces additional moisture equal to the moisture that is removed from the product during the drying process (a drying scheme indicating moisture and heat flows). Therefore, in the drying process, it is also necessary to remove large amounts of heat, which can be transformed into work or used in another process. Figure 8 shows the pressure enthalpy diagram of the ejector heat pump process.

Figure 8: Example of P-H Diagram of Ejector Heat Pump Process

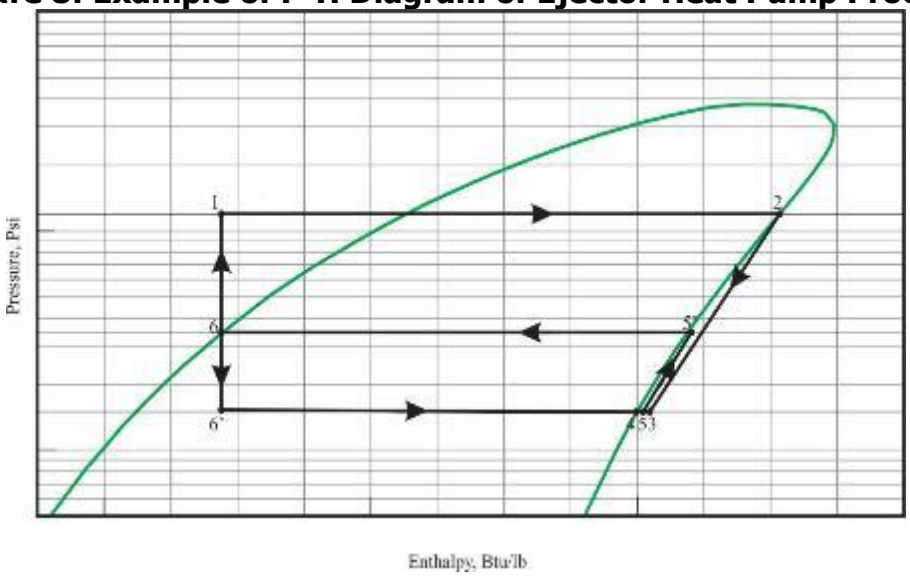

1-2 working flow heating and evaporation in generator, 3-4 working flow expansion in ejector nozzle, 4-5 and 3-5 working and secondary flow mixing in suction chamber, 5-5' – flow mixing and compression in ejector mixing chamber and diffuser, 5'-6 condensation, 6-1 liquid fluid pumping into vapor generator, 6-6' liquid throttling to evaporator, 6'-4 – fluid evaporation in evaporator.

Source: Wilson Engineering

In the vapor compression cycle of a compressor-driven heat pump, only part of the heat of combustion of the fuel is used: heat of combustion is converted into work (electricity), taking into account losses during its transfer and conversion of voltage from low to high, and then lowering the voltage at the consumer. This means that the

real efficiency of the jet heat pump is 1.4—1.8 times higher than that of the traditional one. In addition, the jet heat pump has a large temperature range for its work. The equations supporting this are found in Appendix B.

2.3 Laboratory-Scale Prototype

A laboratory-scale prototype of the system was designed, built, and tested to verify the technology grounds for the project. Drying curves allowed to optimize the drying parameters at the given conditions. Figure 9 shows the prototype dryer used for laboratory verification.

Figure 9: Prototype of Rotary Dryer with Built-In Heat Exchanger

Source: Wilson Engineering

2.4 Advanced Ejector Heat Pump Simulation and Design

2.4.1 System Specifications

The specifications for the industrial advanced drying system were provided by Wilson Engineering Technologies as shown in Table 1, with input from the host site, Martin Feed, LLC. The capacity of the thermo-vacuum drying system (TVDS) is 10 tons of

product per hour. It is designed for drying food wastes with initial moisture content of 35 percent. The final product moisture required by Martin Feed is 10—12 percent. Product temperature during drying should be less than or equal to 50°C (122°F) to avoid any negative effect on product nutritional quality. Product heating is provided by the latent heat released from the steam condensation at specified temperature and pressure conditions as the product goes through the dryer.

Table 1: Design Parameters for 10 Ton/Hour Drying Capacity

Specification	Value
Product weight	80,000 kg (176,400 lb)
Initial moisture content	35%
Final moisture content	12%
Total mass of removed moisture	20,909.1 kg (46,105 lb)
Weight of product batch loaded in rotary dryer	166.67 kg (367.5 lb)
Moisture mass flow rate	0.726 kg/second (1.6 lb/second)
Working steam temperature	270°C (518°F)
Working steam pressure	55.03 Bar (798.14 psi)
Heat input	860.51 kW (2936.15 MBtu/h)
Heat recovery: moisture evaporation from the product	1721 kW (5872.3 MBtu/h)
Water pump power input	3 kW
Rotary dryer drive power input	10 kW

Source: Wilson Engineering

Project design involves the following steps:

1. Heat input and vacuum level parameters optimization, based on previous studies and available drying curves; drying time definition at various vacuum depths achieved in the rotary dryer with waste food mixture.
2. Preliminary design of the rotary dryer with a product moving shaft and heat exchange surface for a single module.
3. Preliminary design of the ejector-based vacuum system and heat pump.
4. Pre-order of off-the-shelf parts and manufacture of the original parts for a TVDS under the field supervision of the project designer's team.
5. Control for installation, check-out and startup operations, and shakedown tests.
6. Tested system improvement, according to the testing results.

7. Monitoring, evaluation, and recommendation for system use; operation manual print-out.

2.3.2 Process and Ejector Simulation

In the first phase of the project, Wilson Engineering Technologies designed the gas-fired thermo-vacuum system. From data provided by the host site, their team developed the heat and material balance simulation for process and instrumentation diagram (P&ID) development to account for all energy flows and product drying principles, based on the system specifications provided.

Based on the results of the simulation, a mathematical model of the vacuum ejectors was developed that fed computational fluid dynamics (CFD) modeling of the vacuum ejector (Figure 10). Wilson Engineering Technologies has a strong background and experience with fluidic ejector compression and developed the advanced heat pump design. The detailed steps and fundamental equations are presented in Appendix B.

Figure 10: Computational Fluid Dynamics Model of Vacuum Ejector Pump

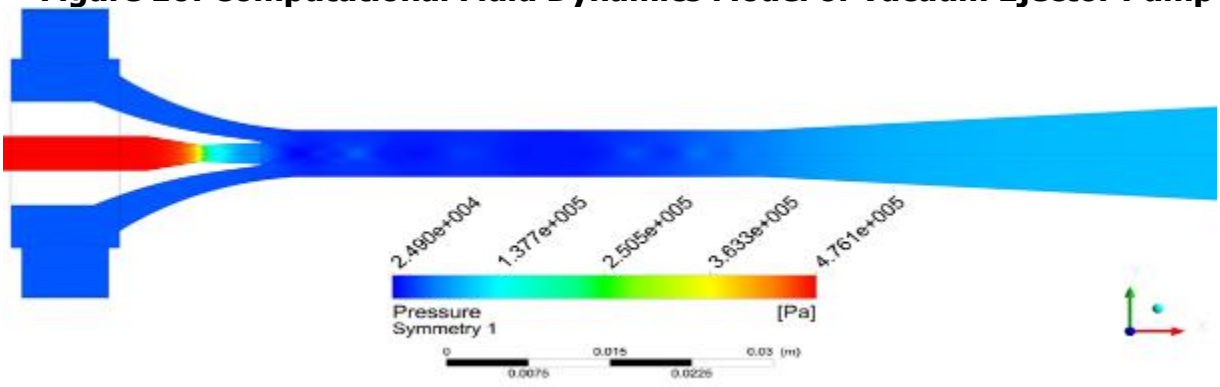

Source: Wilson Engineering

The thermally driven ejector system replaces the mechanical compressor used in traditional heat pump cycles and the vacuum pump used in traditional thermo-vacuum dryers. The replacement of an electrically driven compressor with a natural gas (thermally) driven ejector significantly saves on energy costs, thereby reducing greenhouse gas production.

2.3.3 Process Description

The P&ID for the advanced heat pump gas-fired thermo-vacuum drying system is seen in Figure 11. There are two closed steam/water loops: the boiler loop and the thermal driven ejector/dryer loop. The descriptions following reference the equipment numbers from the P&ID. Additional schematics of the boiler, ejector block, tank, and holo-flite can be seen in Appendix A.

Figure 11: Process and Instrumentation Diagram of Ejector Drying System

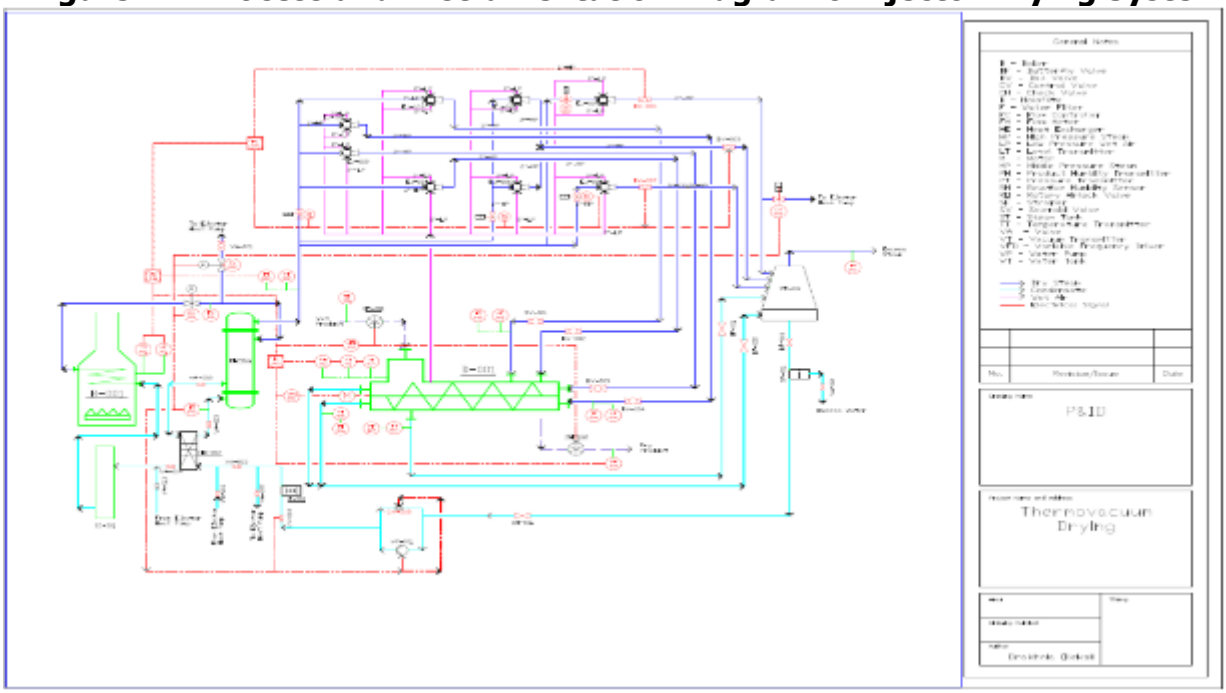

Source: Wilson Engineering

2.3.3.1 Boiler System

The first steam loop is associated with the boiler. The heat pump serving Martin Feed includes a steam generator that receives heat from a Clayton steam boiler. The boiler provides the motive fluid for the ejectors and heat to the product via indirect heating. This boiler can operate in various modes of full or partial load, which makes it possible to easily adapt to specific drying conditions without losing the extra energy resource.

The reason this steam loop is kept separate from the main system is to maintain the integrity of the boiler system by keeping any impurities evaporated from the product out of the boiler tubes. The boiler is supplied with specially prepared water provided for by the requirements of its safe and efficient operation, the stock of which is replenished from purchased containers.

The boiler (B-001) produces saturated steam at 338°F and nominal 200 psi. The steam is condensed in a shell and tube condenser-evaporator (HE-001) as it vaporizes the motive steam for the ejectors, which are on the tube side of HE-001. The condenser-evaporator is a vertical smooth-tube single-pass shell-and-tube apparatus. Process water boils in the tube bundle, and steam from the boiler condenses in the annular space. The condensate from HE-001 goes to a counter-current plate and frame heat exchanger HE-002, which is used to preheat the motive fluid to bubble point temperature. This reduces irreversibility in the heat exchange process and ensures the operation of the condenser-evaporator without pressure and level fluctuations. The sub-cooled condensate completes the loop back to B-001, where it is again vaporized.

2.3.3.2 Thermal Driven Ejector System

The second steam loop contains the thermal driven ejector system, steam tank, and dryer. In this circuit there are certain impurities of salts, fats, and dissolved gases present. This water, before being supplied by the pump to the heat exchanger, is preliminarily cleaned of impurities, the fats separated from it are returned to the product, and all mechanical impurities are filtered. Starting at heat exchanger HE-001, bubble point condensate enters the tube side of HE-001 and comes out as saturated steam at 150 psi (366°F). The steam is routed to the nozzles of eight parallel-connected ejectors (EJ-001, -002, -003, -004, -005, -006, -007, -008). This steam is the motive fluid for the ejectors to entrain the evaporated moisture from the product and recompress it, thereby recovering its useful heat. All ejectors suck off the vapor-air mixture from the vapor space of the holo-flite®, which is released from the dried product due to the heat added. Thus, the ejector takes heat with a temperature of about 70—80°C at a pressure of 60—70 kiloPascal (kPa) and converts it into heat at a temperature of 90—100°C and pressure of 100—115 kPa, i.e., works as a heat pump Additionally, a vacuum is pulled in the dryer, increasing the rate of product drying many-fold. The steam enters the ejector at about 115 psi (347°F). After passing through the expanding nozzle, the pressure is reduced to about 8—10 psi, entraining the product vapor. The combined steam and moisture pass through the ejector, exiting at ambient pressure and with a few degrees of superheat (~215°F). Ejectors can be brought online independently to provide additional capacity depending on the level of product moisture.

The useful heat remaining in the steam exiting EJ-001,-002, -003, and -004 is used to heat the product going through the dryer (D-001), being routed to the dryer jacket and screws. The hollow shaft and flites of the screws are heated by the steam, and that heat is transferred directly to the product as it comes in contact with the screws as it moves through the dryer. If additional ejectors are brought online, the exiting steam is routed directly to the steam tank (ST-001). The steam in the dryer jacket and screws heats up the product to increase the rate of evaporation and condenses in the process. The condensate exiting the dryer is routed to ST-001.

At ST-001, any uncondensed steam and low levels of incondensable material, such as air that may enter with the product, is vented. It was outside the scope of the current project, but future iterations of this system would include a condenser to recover the vented steam to usable condensate. This condensate could be combined with other excess water streams, processed, and utilized for irrigation, livestock, or other uses. Condensate exits the bottom of ST-001 and is pumped (WP-001) through a water filter (F-001) before completing the loop to be regenerated to steam. The condensate is first brought up to boiling point temperature through HE-002, and then boiled in HE-001.

2.3.3.3 Product Dryer

The product path through the dryer turns high moisture feed to low moisture product. The wet product enters the top of the dryer through a rotary airlock valve (RO-001)

that meters feed into the dryer without leakage of air into the vacuum. In the dryer, the product temperature is raised to about 180°F through contact with the heated screws and jacket as it is continuously moved through. Heat and vacuum (8-10 psi) result in very rapid evaporation of product moisture. The dryer should be operated fully loaded to ensure full contact of the product with the sides and screws of the dryer, which are heated with steam. The dry hot product exits the rotary dryer at the other end from the bottom through another rotary airlock valve. The moisture of the product is controlled through the speed at which it is moved through the dryer, and monitored through product humidity transmitters at the entrance and exit of the dryer.

2.3.4 Working Fluids and Operational Parameters

The main working substance in the current drying system is water and water vapor. When creating a vacuum in the holo-flite space in the first stage, the amount of air will prevail, but later, since air infiltration is minimal, the steam-water component of the vapor-air mixture increases. As the product moves along the holo-flite at nominal or lower initial humidity, the added mass in the ejectors decreases. This automatically leads to a decrease in pressure in the holo-flite cavity. A further decrease in pressure stimulates more intensive removal of moisture, which can lead to overdrying of the product. When such a situation arises, the steam supply to the ejectors nozzle temporarily stops; all other parts will be stopped automatically in a short time, calculated in 10—20 seconds. If the initial humidity of the product is outside the allowable values, and the pressure in the holo-flite cavity does not reach the calculated value of 70 kPa at the exit of the holo-flite, operators can reduce the speed of movement of the product along the holo-flite and produce maximum moisture vapor from the product. In extreme cases, when this does not solve the problem, the product from the holo-flite is unloaded and reloaded onto the input.

Listed below are the results of the calculation of the entrainment ratio, the coefficient of performance (COP), the geometric characteristics of the flow part of the ejector with the flow of working steam 1kg /s, as well as the values of a number of thermodynamic functions of the working, ejected, and mixed flows:

MolarMass=18.0153; TTP=273.16;

NormalBoiling=373.124; AcentricFactor=0.3443

Tr=443.15 Tc=376.15 Ti=363.15К

Pr=792.187 Pc=112.768 Pi=70.1818Па

Ror=4.12219 Roc=0.660564 Roi=0.423898 кг/м3

Kr=1.39184 Kc=1.33801 Ki=1.33386

Hr=2767.9 Hc=431.827 Hi=2659.53кДж/кг

Rr=16.0554 R3=59.2024 Rr1=23.631 R2=83.7248 Rc=274.018 Lc=187.383 мм

EntrRat=1.0256 Upr2=6.92862 Upr1=1.07498 Upr3=1.0256 F3/Rf=13.5968

COP=0.978024

Temperature after ejector = 392.032К

The operation of the heat pump on water vapor in a given temperature range is characterized by good performance characteristics: low pressures in the steam generator and condenser, explosion and fire safety, and non-toxicity and total environmental safety (ODP [Ozone Depletion Potential] = 0; GWP [Global Warming Potential] = 1). In this case, most of the water and water vapor circulate in a closed circuit. Excessive water extracted from the products during the drying process can be accumulated and used for the necessary technological or secondary purposes. The circulation circuit of the boiler water is isolated from the circulation circuit of the polluted working water, which significantly reduces operating costs for water treatment. Losses from under-recovery are relatively small due to high heat transfer coefficients in both the condensation process and the boiling in the condenser of the steam generator, which is also determined by the positive properties of water as a highly efficient heat carrier.

Compared to hydrocarbon-based low-boiling substances, water has a higher viscosity, which simplifies the requirements for seals at joints and minimizes leakage. In addition, due to the availability of water and its safety, small leaks are acceptable and easily replenished from the accumulated reserve.

2.3.5 Integration Features

This thermal vacuum method of drying the product is based on the principle of operation of an ejector heat pump. In this case, the heat pump can be a simple single version with a single splitting of the heat flux, as well as a double one with additional heat pump circuits that can locally increase the potential of exhaust heat to a higher level, increasing the overall efficiency of the system. Figure 12 gives schematic diagrams of two alternatives for the inclusion of heat pumps into the dryer circuit.

Figure 12: Schematic Diagram of Two Variants of Heat Pump Connections

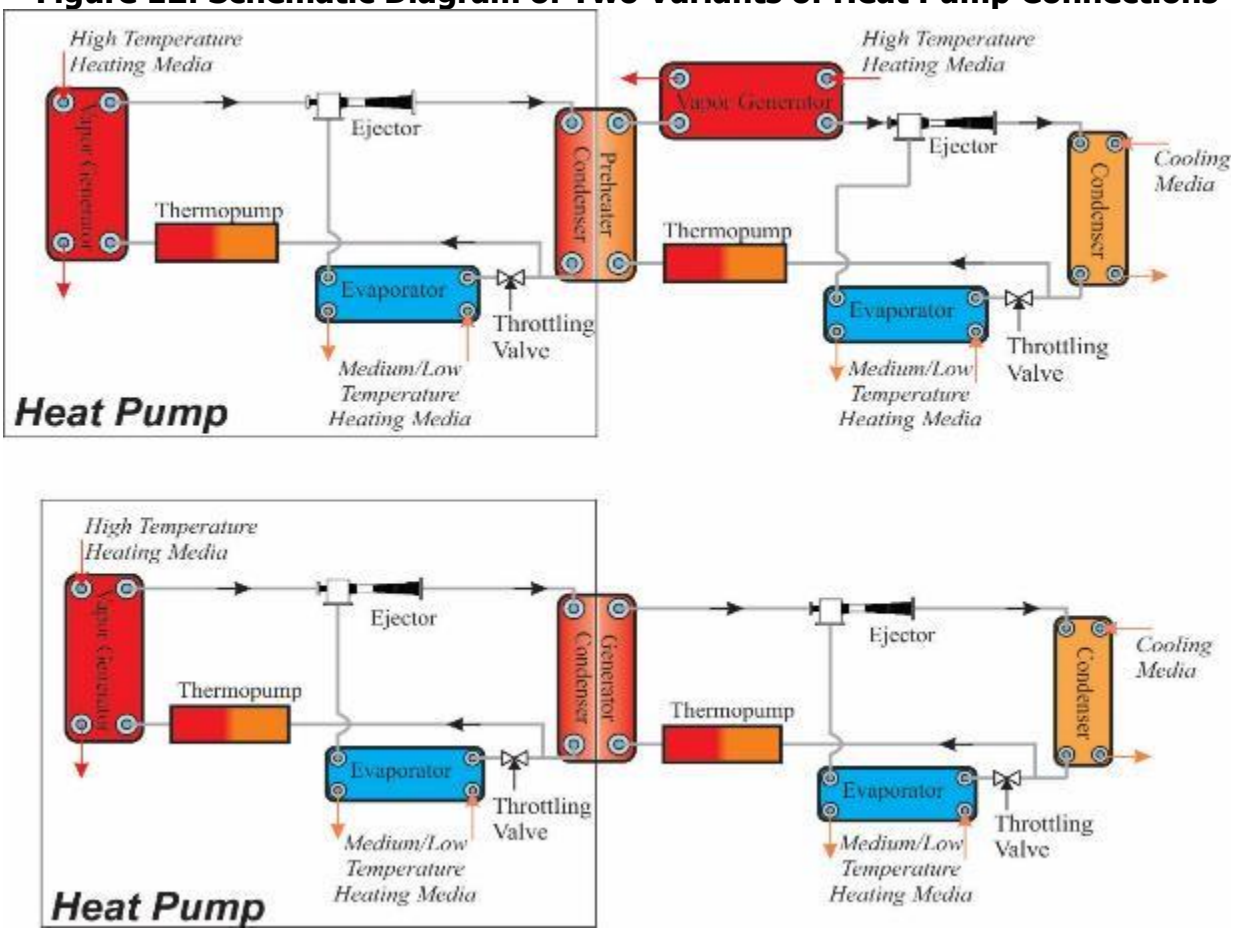

Source: Wilson Engineering

An ejector heat pump consumes high potential heat from a gas boiler, takes heat from a source with a low temperature (the vapor-air mixture from the product being dried), and releases heat to the intermediate potential in an amount equal to the sum of the heat removed from the boiler and from the product. Since in our project these quantities of heat are about the same (COP=1), then at the output we get a doubling of the heat taken from the boiler. Half of this heat goes to heat the product, and the other half remains unused in the process.

MolarMass=18.0153; TTP=273.16;

NormalBoiling=373.124; AcentricFactor=0.3443

Tr=443.15 Tc=375.65 Ti=363.15

Pr=792.187 Pc=110.807 Pi=70.1818

Ror=4.12219 Roc=0.649812 Roi=0.423898

Kr=1.39184 Kc=1.33783 Ki=1.33386

Hr=2767.9 Hc=429.716 Hi=2659.53

Rr=16.0554 R3=60.2438 Rr1=23.6327 R2=85.1976 Rc=278.752 Lc=192.295

EntrRat=1.06208 Upr2=8.36953 Upr1=1.12034 Upr3=1.06208 F3/Rf=14.0794

COP=1.01286

Temperature after ejector = 391.465

The drying process is a non-stationary process, because as the product moves along the holo-flite, the moisture content changes. Local areas of airspace above the product also have different moisture content, which may contribute to the migration of air flow along the product. In the continuous process of product receipt, it is not possible to reduce the pressure above it; space is solid. It is not possible to divide this space into hermetic compartments due to the continuous movement of the holo-flite. If the drying is carried out discretely or the holo-flite is performed as several consecutive chambers, isolated from each other holo-flite, then a deeper drying can be carried out. At the same time, the pressure can vary up to 0.1 bar. Unlike operation in off-design conditions, when a decrease in the ejection coefficient is a consequence of a change in operating parameters, in this case a decrease in the flow rate of the ejected medium causes a decrease in the suction pressure, while the ejector continues to operate at the limiting mode. Thus, the modeling of the ejector for the conditions of maximum initial humidity of the product allows, without changing the geometry of the flow part, to work in optimal conditions at the limiting mode at any values of the initial humidity below the maximum. This means that in the ejector with any parameters there will be no locking of the cross-section of the mixing chamber, reverse currents, i.e., unproductive losses. Otherwise, this would lead to the return of water vapor to the holo-flite cavity and wetting of the product, which is unacceptable. Figure 13 represents the dependence of evaporation temperature, evaporation pressure, and ejector outlet temperature on entrainment ratio.

Figure 13: Evaporation Temperature, Pressure, and Ejector Outlet Temperature vs Entrainment Ratio

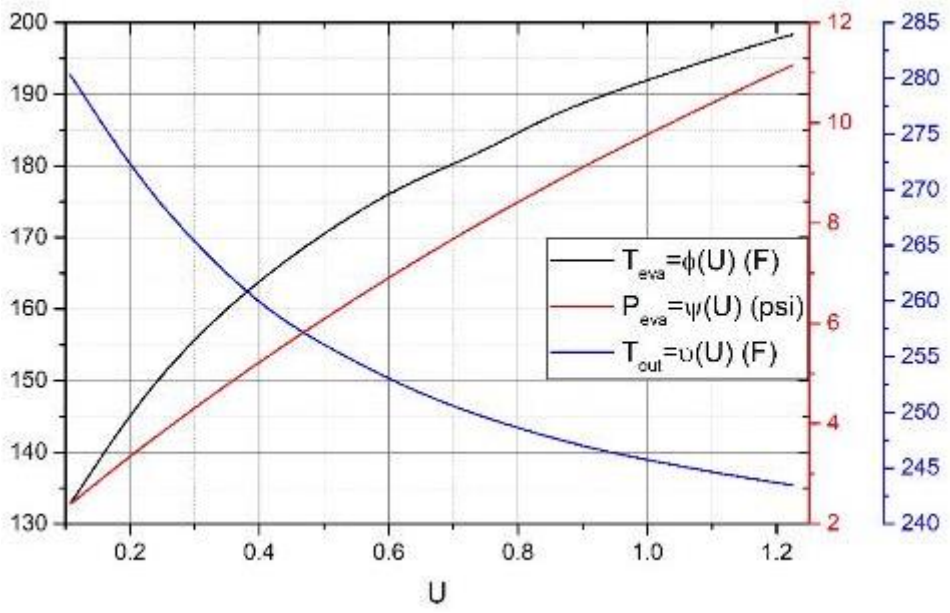

Source: Wilson Engineering

The final installation of thermal vacuum drying is the layout of the following main components:

- Clayton steam boiler with a capacity of up to 200 BHP of heat, which produces high pressure steam and temperature to provide heat generation of the working steam
- Heat exchange unit used to generate steam, consisting of a series-mounted countercurrent plate water heater and a vertical shell-and-tube steam generator condenser developed by Wilson Engineering Technologies, Inc.
- Holo-flite® with a double horizontal screw of the company "Denver," upgraded to the objectives of this project
- A set of 8 Wilson-designed ejectors connected in parallel into groups of 1, 2, and 4
- The product charge unit, consisting of a feed hopper and an inclined auger and electric motor
- The product discharge unit, consisting of a receiving hopper and an inclined auger, feeding the product into the dried product storage area
- Separator-battery of steam-water mixture, from which water is supplied to the heat exchange unit of the steam generator

The operation of the drying unit is controlled by a separate controller mounted according to the scheme developed by Wilson Engineering Technologies, Inc. The operation of the boiler is controlled independently.

2.4. Performance Evaluation

The demonstration system installation scheme allows varying the performance in a fairly wide range by changing the speed of the auger supplying product through a change in the frequency in the range of 75 to 10 hertz (Hz).

The thermal load was regulated by the number of ejectors switched on and the self-regulating pressure on the suction line of the ejectors. The boiler regulates its performance by the amount of heat consumed in the production of steam in the shell and tube heat exchanger.

In cases where the initial humidity of the product has a maximum design value of 35 percent, the product feed rate is minimal and corresponds to the minimum engine speed, i.e., minimum current frequency. The maximum performance of the product is 366 lb per minute. In this case, the final moisture content of the product is 12 percent. Accordingly, with a lower initial moisture content of the product, the product performance can be increased in accordance with the amount of moisture that must be removed from the product to a fixed final moisture content.

Table 2 presents the values of the maximum mass productivity of the installation and the speed of rotation of the holo-flite, depending on the initial humidity of the product.

Table 2: Mass Productivity of the Dryer at Various Initial Moisture Levels of the Product

	Initial moisture, %	Product flow, lb/min	Frequency, Hz
1	35	366	22
2	32	424	26
3	30	467	31
4	27	560	38
5	25	647	42
6	20	1051	46
7	17	1682	55

Source: Wilson Engineering

It should be noted that the GFTD installation designed and demonstrated during this project is not intended for drying of over-wetted product, as there is an increased adhesion of the product (consisting mainly of carbohydrates) to the surface of the holo-flite®, producing an over-dried crust which is required to be removed for optimal

operation. Therefore, during the pre-commercial engineering and thermo-vacuum technology implementation, the product should either be pre-dried (or pressed) to the level of at least 50 percent moisture content, or the heating surfaces should be coated with non-sticking material to prevent undesirable depositions.

CHAPTER 3:
Full-Scale System: Installation, Startup, and Shakedown at Host Site

The advanced drying system was proven in a laboratory setting and design and simulation supported the promising energy savings anticipated through this technology. Demonstration in the field was the next step in proving the technology benefits. Figure 14 shows the final system layout of the dryer installed at the participating host site.

Figure 14: Schematic of Gas-Fired Rotary Thermo-Vacuum Drying Demonstration System

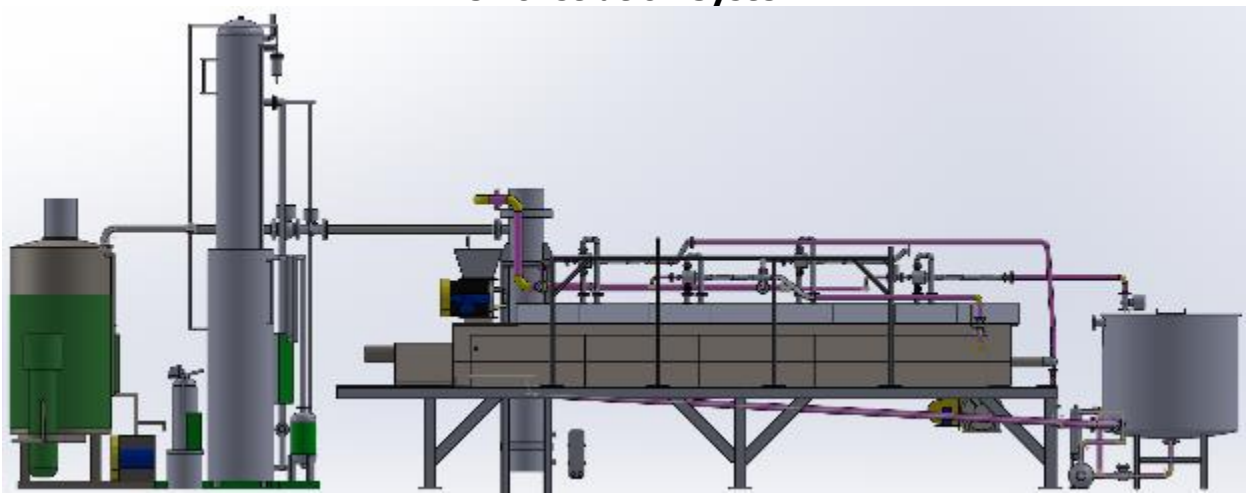

Source: Wilson Engineering

The demonstration size was defined as a full-scale commercial capacity of 100 tons of product per day with approximate gas load of 6-7 MMBtu/hr.

3.1 Host Site: Martin Feed, LLC

The proposed effort was originally hosted by one of the major California food processing companies, Inland Empire Foods (IEF). Inland Empire Foods was selected as a qualified Southern California-based food processing facility with representative drying operations. IEF is a premier manufacturer and supplier of quality flaked and whole legumes. Since 1985 IEF primarily produces dehydrated refried beans, so cost-effective and energy efficient drying technology is of IEF's great interest. However, this site was unable to participate, and a new site was identified. During the review of the original rotary drying system layout, Inland Empire Foods withdrew from participation due to concerns over assuming the anticipated loss of product during startup, shakedown, and demonstration. GTI identified an alternate demonstration site, Martin Feed, LLC in Corona, California. The feed quantity for the new host site was significantly higher than

for IEF, initiating the change in the dryer design from the drum style initially proposed to a screw-type dryer.

Martin Feed, LLC is a family-owned and operated feed business. The Martin family began in the bakery waste industry in the 1960's when Frank E. Martin Sr. started collecting waste to feed his cattle. Martin Feed collects waste bakery material and sells the processed product to dairy farms throughout California. The process starts with the collection of materials from facilities that generate waste bakery products. Such products include bread, dough, crackers, pastries, pies, tortillas, and cookies. The collected material is transported to the process yard located at 8755 Chino-Corona Road in Corona, California, where all packaging is removed and bakery-material is placed on a slab of concrete to be sun dried. Once dry, the materials are mixed together and ground in an industrial grinder. During the fall and winter months, when rain and moisture averages are above an inch of rain and often above 2.5 inches of rain, the production is curtailed, as it takes longer to dry the product to the desired moisture content for grinding operations. The site is located within the South Coast Air Quality Management District. Figure 15 shows feed product samples from Martin Feed before and after grinding.

Figure 15: Martin Feed Product Samples

Dryer input (left) and final product after grinding (right).

Source: GTI

The purpose of the dryer designed for Martin Feed is to provide product at 12—15 percent moisture, which is optimum moisture content for pulverizing the cattle feed for storage and sale. The feed is loaded into a hopper, travels up an auger, though an airlock valve, and into the holo-flite® for drying. The dried product exits the holo-flite® through a rotary airlock valve and is stored in the loading area. The starting product contains an estimated 35—45 percent moisture. The rate of drying to achieve optimum moisture will be determined by the process rate. The estimated process rate under ideal conditions using the thermo-vacuum dryer is one minute per 160 pounds of dried product. The process rate is dependent on the initial product composition.

3.2 Field Engineering and Installation

Upon completion of the series of pre-shipment tests, evaluations, and inspections, all the components of the demonstration system were delivered to the participating host site for final assembly and installation. In addition to typical inspections, the rotary heater components were pressure tested prior to shipment to the site. The team and local mechanical installation contractors performed extensive field engineering. The host site provided the space for the unit; however, it was not able to provide the required utilities, namely power, water, and gas. No construction permit was required, as a skid-mounted approach was elected for the demonstration unit. Figure 16 below shows various delivered system components at the host site ready for assembly. Figure 17 shows the mechanical installation of the various components, which are described in more detail in subsequent sections, and Figure 18 shows an overall view of the installed system.

Figure 16: Delivered System Components

Overview of the Rotary Dryer (Top); Delivered wrapped boiler package components (Bottom left); Project team and a process ejector assembly (Bottom right)

Source: GTI

Figure 17: System Mechanical Installation at Martin Feed, LLC in Corona, California

Source: GTI

Figure 18: Overall View of Thermovacuum

Drying system installed at the site (Top), main control panel (Bottom left); ejectors (Bottom right).

Source: GTI

3.2.1 Utilities

The host site did not have hookups for power, water, gas, and compressed air. A generator was procured for startup, shakedown, and demonstration periods, and natural gas was supplied by a mobile natural gas supplier, Ultimate CNG. Soft water totes were procured for charging the system for startup. A mobile air compressor was rented to supply air for instrumentation.

3.2.2 Steam Generator

Clayton Industries was selected to provide the steam generator for the system. This steam generator provides steam for indirect heating of the motive fluid to drive the ejectors.

3.2.3 Airlocks

Prater's rotary airlocks were used for feed handling to charge and discharge the product into the system that is under vacuum. The airlock at the product inlet side feeds the

product into the vacuum in a metered manner while maintaining the pressure differential through an airlock seal, thereby preventing loss of vacuum and temperature in the system. The same airlock operation was established at the product outlet. Appendix C includes photographs of the airlock used in the demonstration unit.

3.2.4 Rotary Holo-flite®

Metso's rotary holo-flite® was specified for the continuous integrated heating and transportation of the product. Figure 19 shows an overall view of the holo-flite® configuration by which product can be moved through a trough. Multiple shafts can be integrated for larger feed rates. It is comprised of a jacketed cylinder containing screw conveyors. The rotary transport unit selected for the project has two screws, which enables transport of the required 100 tons per day of product requested by the host site.

Figure 19: Generic Holo-flite® Illustration

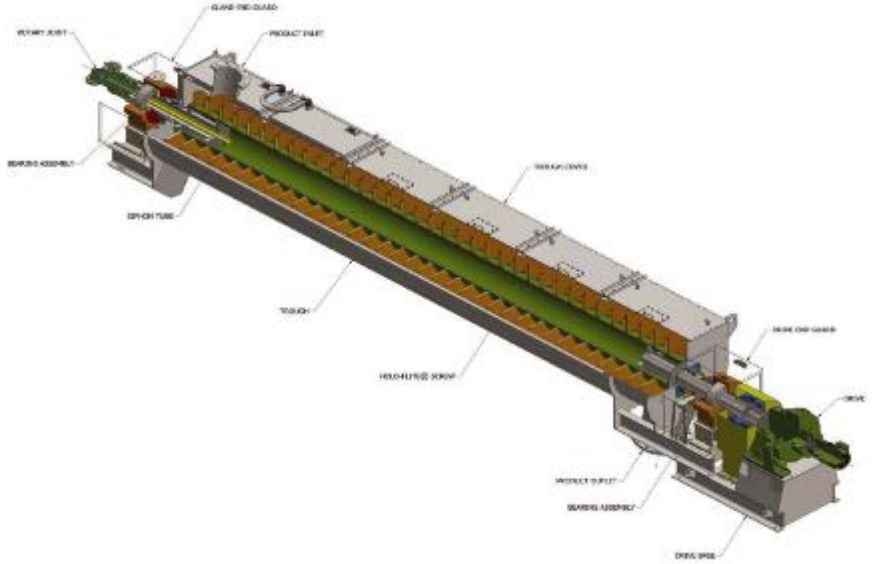

https://www.metso.com/products/dryers-and-coolers/holo-flite/

Source: Metso

This is an established thermal drying technology that has been used in various industries for over 60 years, including food processing, petrochemical processing, mining applications, and waste applications. The benefit of this technology is that it continuously conveys product through a trough via rotating screws while the product is indirectly heated as it comes into contact with the hollow flights and shaft. It is an indirect thermal heating/drying system. The inside of the shaft of the screw is hollow, allowing for the flow of a thermal fluid, as seen in Figure 20. For this application, steam is used as the thermal fluid. The trough and screws are constructed of stainless steel.

Figure 20: Rotary Holo-flite®

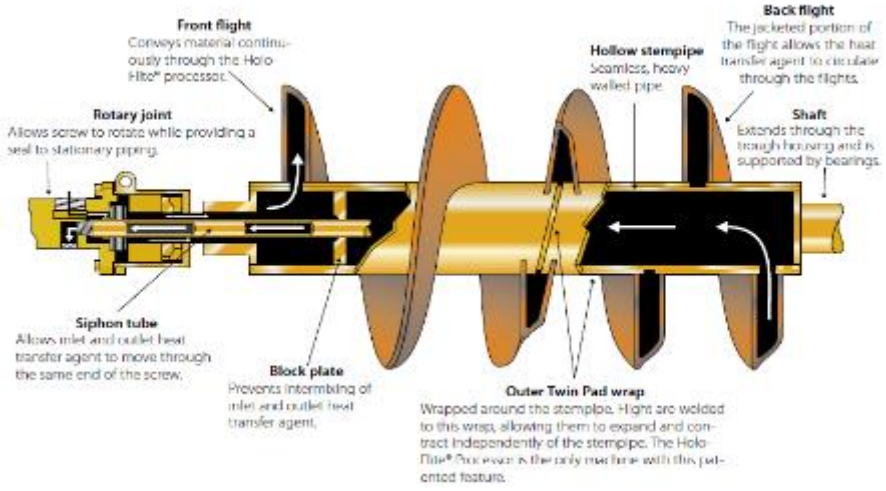

Source: Metso, manufacturer

3.2.5 Ejectors

As described previously, the ejectors create a dynamic vacuum in the dryer chamber and act as a fluidic compressor for the advanced heat pump. The specifications were provided for the motive and ejected flow-operating regimes. Figure 21 shows the vacuum ejector assembly, and Figure 22 shows the assembly of the ejector-based system.

Figure 21: Vacuum Ejector Assembly

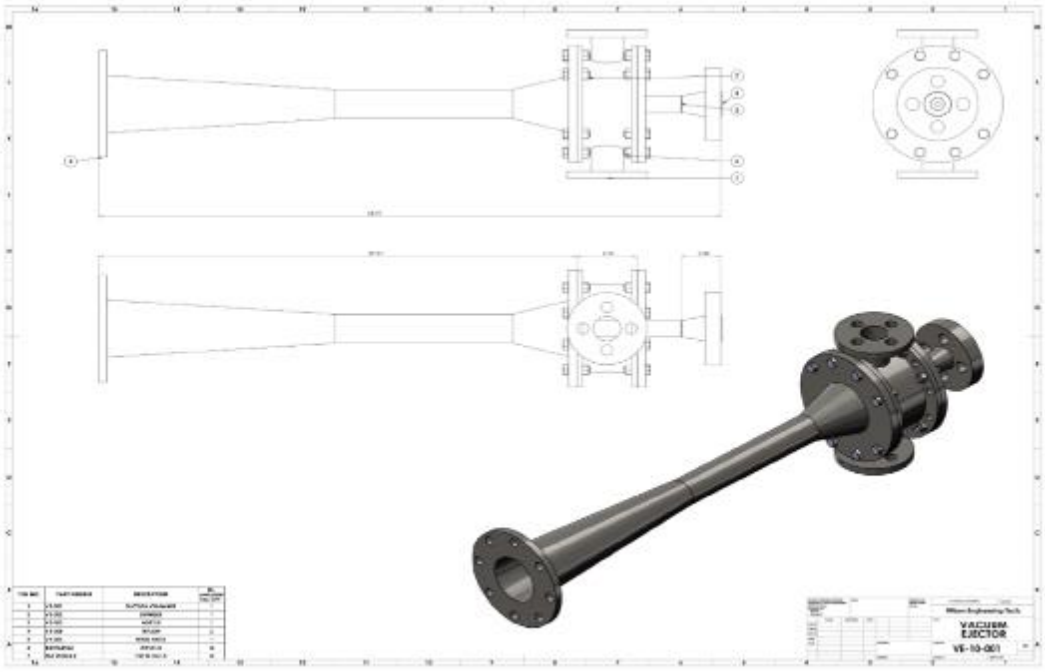

Source: Wilson Engineering

Figure 22: Assembly of Ejector-Based System

Source: GTI

3.2.6 Measurement Sensors and Control Panel

The combustion controls were integrated into the packaged boiler unit supplied by Clayton Industries. In commercial implementation of the system, the boiler controls will be fully integrated with the steam controls of the ejector system.

The dryer controls for the demonstration effort were developed by Spurt Electric, Inc. The controls are used for GFTD motor control of the various motor components and ejector solenoid valves to maintain desired product rate through the dryer, condensate recirculation, vacuum level, and heat level in the dryer. These are described in more detail in Appendix D.

The overview screen shown in Figure 23 presents an overall picture of the GFTD, including temperatures, pressures, and rotation speed of the inlet/outlet airlocks and holo-flite® screws.

Figure 23: Control System Overview Screen

Source: GTI

The solenoid valves control screen (Figure 24) allows the operator to open and close valves controlling the level of vacuum in the dryer and to direct steam to the dryer jacket and flites to apply heat to the product.

Figure 24: Solenoid Valves Control Screen

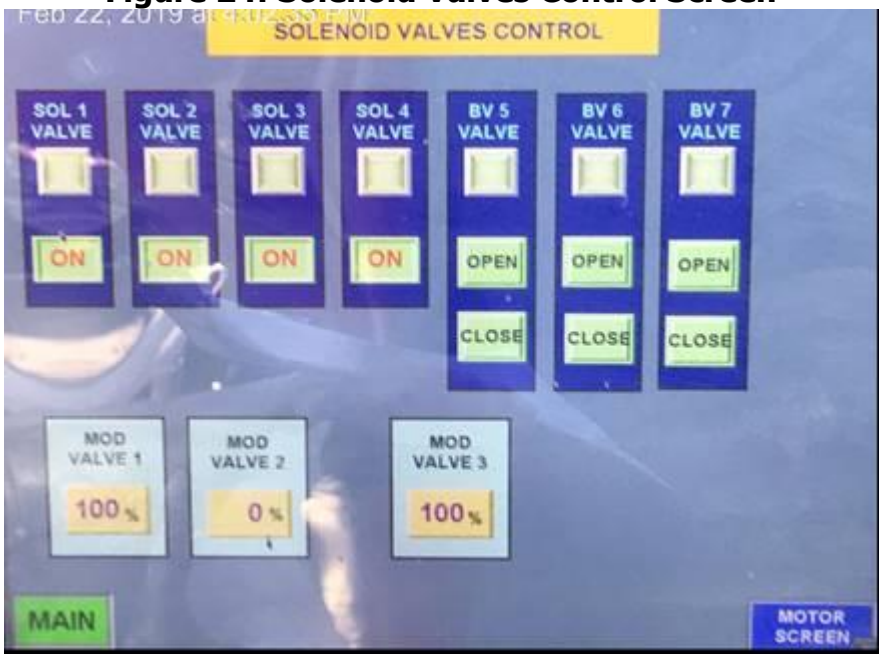

Source: GTI

The motor control screen (Figure 25) allows the operator to adjust the speed of the airlocks at the inlet and outlet of the dryer and to change the holo-flite® speed, which is a variable that can affect the level of drying of the product during the test run.

Figure 25: Manual Motor Control Screen

Source: GTI

The full control system was not in place for the demonstration system. The completed system will have feedback from the humidity sensors at the inlet and outlet of the dryer to control the speed of the system and the vacuum pulled, and to automatically adjust to meet product moisture targets.

3.3 System Startup

3.3.1 SCAQMD Compliance Testing

Once the boiler and dryer were installed, compliance source testing for SCAQMD permitting followed the system startup. Photographs from the startup and compliance testing are shown in Appendix C.

3.3.2 System Shakedown and Adjustment

Once the system was assembled and the initial startup and compliance testing was complete, the host site integrated the product charge and discharge hardware, consisting of hoppers and augers (Figure 26).

Figure 26: Feed System

Source: GTI

During the system shakedown some technical failures were identified, such as steam leakages and failed components and control sensors, which had to be corrected prior to main data collection. New sensors were calibrated, product handling equipment (Prater Air-locks for charging/discharging) was adjusted, and the main motor, sprocket, and gearbox were replaced to ensure the required production rate during the performance data collection, with special attention given to ensuring stable torque for wet and heavy product processing.

Besides a few leaking couplings that were easily replaced, the pipe lines, steam generator-condenser, and plate heat exchanger worked as designed and required no adjustments or repairs during shakedown.

CHAPTER 4:
GFTD Performance Data Collection

Upon completed shakedown, the system performance was evaluated. Heavy rainfall in the Corona area and mechanical repairs to the dryer unit postponed this effort multiple times. The goal was to run the GFTD at production rates and collect performance data on its operation. The data was collected from the deployed demonstration drying system for evaluation and comparison against state-of-the-art specification.

4.1 Measurement and Verification Scope

The program's quantitative performance objectives for the thermo-vacuum dryer method are listed in Table 3.

Table 3: Program Quantitative Performance Metrics

Performance	Metric	Data Requirements
Fuel efficiency	Fuel usage and/or fuel use per ton product	Fuel rate and process rate during process operation
Emission rate	NOx, CO, O_2, and GHG concentrations	Boiler flue gas measurement – per SCAQMD permit requirements
Steam rate	Amount of steam used per ton product	Steam rate during process operation (calculated from fuel rate)
Process rate	Amount of product dried per period	Product weight and time required to dry product
Moisture removal efficiency	Percent moisture removal	Percent moisture removed and quality of finished product
Energy consumption	Total energy used to process ton product	Fuel, electrical, and water demand during operation

Source: Tetra Tech Inc

Tetra Tech served as the independent measurement and verification (M&V) contractor for the project. The full M&V report, contained in Appendix E, describes the methodologies used for fuel, emissions, product moisture, and energy and mass balance calculations.

4.2 Demonstration Testing

Not all connections and controls shown on the P&ID were included in the field unit. The automation of the process has not yet reached the planned level, and a number of operations were performed manually. This was caused by the need to more carefully manage the process control algorithm prior to arranging remote operations. Tuning during the run occurred when parameters went off design, but tuning should not be required once the system is fully automated.

Data collection was challenging due to mechanical issues with the unit that prevented long runs and required a much longer timeframe than available for repair and adjustments. Finally, the project team managed to complete scheduled data collection under very challenging circumstances, with adverse weather conditions; continuous rains with hail and even snow in Southern California, accompanied by strong wind, made it difficult to run the demonstration system in an outdoor area. The extremely wet product resting in the holo-flite® from the wet weather initially clogged up the outlet airlock, requiring it to be removed, unclogged, and reinstalled. For the reliable operation of the drying system, it is strongly recommended that a shed should be installed over the product feed in order to eliminate the negative effects of weather conditions.

Ultimately, several short runs were performed to collect data. The runs confirmed that the ejectors operated as planned to lower the pressure of the holo-flite® drying volume as well as to preheat the product with the condensing steam.

4.2.1 Operation

For the demonstration testing, the holo-flite® and feed auger rotation were set to process 166 kg/minute of feed with initial moisture content of 35 percent. The total time for product to pass through the dryer based on the settings was 2.5 minutes (13 rpm and a flite step of 0.2 meters, with the total length of the holo-flite® at 6.5 meters). These system parameters were initially pre-set and ideally do not require any special operating approach once the system reaches the on-design mode.

The boiler started first and generated the required amount of steam to the condenser-generator, where it condensed and evaporated the counter flow condensate from the water tank supplied at the designed flow rate and pressure. Once the design parameters were achieved, ejectors were actuated and product was fed into the holo-flite®, starting the thermo-vacuum drying process.

Feed was loaded to the hopper with a tractor and fed to the airlock via inclined auger. The rate had to be carefully set to avoid jamming of the airlock.

The pressure within the dryer reduced as designed. Table 4 shows the decrease in pressure over the course of the demonstration run.

Table 4: Pressure in Holo-flite® During Demonstration Run

Run Time (Seconds)	Pressure in Holo-flite® (kPa)
90	95
135	70
150	45

Source: Wilson Engineering

The temperature in the holo-flite® remained at 85—90°C for most of the length of the dryer, and then decreased to 60°C in the final quarter of the holo-flite® prior to discharging. Further decrease of pressure led to the temperature decrease in the holo-flite®'s cavity and served to protect the outfeed airlock from thermal expansion. Stabilization of the temperature at the outfeed airlock zone prevented the device from jamming and enabled the designed product capacity to pass through.

The steam generator-condenser and plate heat exchanger performed as designed. Protective filter mesh on the suction ports of the ejectors prevented the product evacuation from the holo-flite® cavity and worked well during operation.

The characteristics of the feed pump installed during shakedown suited the selected operational parameters. The pressure and the condensate return flow rates were maintained and logged by a pressure gauge and an ultrasonic flow meter installed specifically for the demonstration (Figure 27).

Figure 27: Ultrasonic Flow Meter and Condensate Pump

Source: GTI

During the system operation the condensate filter was required to be frequently replaced due to clogging (on the condensate return line). Mesh of 1 micron, 5 micron, and 10 micron size was used in the filter. However, volatile particles from the product and dirt that contaminated the condensate clogged the filters quickly and prevented the condensate pumping at the designed flow rate and pressure. The optimal size of the condensate filter mesh should be experimentally determined. This issue can also be resolved by close-looping the steam condensation to avoid any contamination of the condensate.

Although the ejectors were working as designed, lowering the pressure in the holo-flite®, when heat (steam) was applied to the jacket and shaft of the dryer, the final product did not present any dryer than the feed. It is assumed that there were internal leaks in the jacket or in the screw, and that steam penetrated into the product in liquid phase. The leak path could be in the tail section of the dryer, close to the outfeed. Considering the material of the holo-flite®, as well as the presence of a large amount of oxidation products that were removed during the washing process, it is assumed that there were microcracks or poor quality gaskets. During the trial launches of the ejectors, they worked for some time with the suction windows closed. In this case, the dynamic pressure, converted into static pressure, could also contribute to the leakage in the holo-flite®'s cavity.

The moisture that entered the product, most likely close to the outlet, did not have enough time to evaporate, and re-wet the product as a result. In the follow-on pre-commercial engineering phase it would be necessary to ensure the drying cavity is perfectly sealed and pressurized for at least 10 to 15 days.

4.2.2 Challenges

Besides the challenges addressed above, there were several main reasons contributing to the short lengths of the demonstration runs:

- Boiler modulation was frequent and unstable, resulting in steam pressure and flow rate fluctuation critical for ejector operation.
- Boiler design was not intended for outside operation. Air filter clogging and electronics and burner failure had to be addressed prior to test runs.
- Product infeed and outfeed flow rates that were not properly optimized with existing hoppers and augers caused overloading of the motors, packing the airlocks and preventing its path forward.
- Condensate filter clogging as described above was a cause for immediate shutdown of the system as the pressure and flow rates decreased to a point that affected ejector operation.

As mentioned earlier, there are compelling reasons to assume that the holo-flite heating cavities were not tight enough to steam at elevated pressures. Though some minor

leakages were located and fixed, the exact place for the main pressure drop will only be possible to locate upon a complete inspection of the holo-flite.

At the same time, the results revealed the potential to consider another type of boiler, and identified the necessary design adjustments of the holo-flite and its supporting units.

4.3 Results

The main achievement of the system runs is demonstration of the high level and quality of the calculation, design, and manufacturing of the ejectors, which consistently produced the calculated parameters and automatically shifted to the designed limit load corresponding to the lower suction pressure. The results of the runs have successfully proved that the demonstrated technology can evacuate the moisture from the product with simultaneous product heating and heat pumping effect for efficient drying of product.

4.3.1 Fuel Efficiency and Emissions

A Clayton, Model EG204-FMB, boiler equipped with a low NOx burner was used to generate steam during the drying process. The boiler is rated at 81.5 percent efficient. Emissions testing was performed on the boiler to measure emissions of NOx, CO, and oxygen (O_2) and to demonstrate compliance with the requirements of SCAQMD Permit to Operate and Rule 1146. The average measured CO concentrations were below the quantifiable range of reference method during each test.

Testing was conducted while the boiler was operated at high, mid, and low firing rate conditions. Results are summarized in Table 5. These measurements were taken during the initial startup of the unit and were not repeated during performance testing.

Table 5: Boiler Emission Summary

Parameter	Units	100 Percent Load	50 Percent Load	25 Percent Load
O_2	%	11.30	11.24	11.76
CO_2	%	5.58	5.54	5.24
NO_x	ppm@3%O2	7.53	7.26	6.91
	lb/hr	0.061	0.033	0.015
CO	ppm@3%O2	<18.6	<18.5	<19.6
	lb/hr	<0.092	<0.051	<0.026

Source: Tetra Tech Inc

Boiler emissions are compliant with SCAQMD emissions requirements.

4.3.2 Energy Use Summary

The energy use for the thermo-vacuum system was calculated using direct measurement data and operational data, summarized in Table 6.

Table 6: Energy Use Summary

Source	Btu/hr
Boiler	4,194,240
Steam tank loss	297,085
Condensate return line	1,732,556
Portable generator	N/A

Source: Tetra Tech Inc

4.3.3 Moisture

Moisture analysis was performed onsite using Method ASTM D2216 – 10. The drying time used in the analysis was set at 110F to avoid burning the sample during the moisture analysis process. Results from the analysis are summarized in Table 7.

Table 7: Moisture Analysis

Sampling	Sample Location	Sample Time	Average Moisture, (%)
1	In	11:09	22.39
	Out*	-	14.8 (a) 9 (b) 4.8 (c)
2	In	14:51	18.61
	Out*	-	10.4 (a) 4.6 (b) 0.5 (c)

***Sample moisture at the system outlet has been calculated based on the measured vacuum level, heating input and number of operated ejectors (a – 2, b – 4, c – 6). Actual measurements of outlet moisture were negatively affected by adverse weather conditions during the test and excluded from reasonable consideration.**

Source: GTI

CHAPTER 5:
Project Findings and Recommendations

5.1 Results Summary

The overall aim of this project was to design and demonstrate a high-productivity integrated gas-fired drying technology of superior energy efficiency and benefits, including reduced gas consumption and an accelerated drying process. This system has demonstrated a promising performance at the laboratory scale. Additionally, the main achievement of the demonstration system was the design and manufacturing of the ejectors that are key components of the technology; during the performance testing these ejectors consistently produced the calculated parameters and automatically shifted to the designed limit load corresponding to the lower suction pressure. The pressure measurements clearly demonstrated the ability of the designed system to evacuate the moisture from the drying volume with simultaneous product heating and heat pumping effect for an efficient drying process.

Effectiveness and efficiency of the drying process is basically characterized by the drying time, energy consumption, and capital and operating costs, as well as by product quality and environmental compliance. The thermo-vacuum process significantly improves the operation's drying time and energy consumption, and provides favorable environmental impact to the community.

The project demonstrated the designed performance of the ejector system for product throughput of 366 lb per minute (~11 ton per hour). The ejectors evacuated about 85.9 lb per minute of air-moisture where the air mass portion was under 1.5 percent. However, taking into account the minor leakages in the sealed chambers, the nominal moisture evacuation rate by ejectors should be 47.5 lb per minute to provide the dried product moisture content at the designed level of 12—15 percent.

The parametric optimization of the drying process by considering the product type, throughput variations, and vacuum dynamics are the subject of follow-on efforts.

In order to dry product from 35 percent to 12 percent moisture content, there is a need to remove 84 lb of moisture per minute. For that purpose, it is necessary to heat the product by providing 5.4 MMBtu/hr. The removal of the evaporated moisture would require additional heat for blowing 2,500—3,500 cubic feet/hour (CFH) of air at a temperature of 212—266F in the amount of 10—15 MMBtu/hr. Therefore, the basic estimate clearly indicates a required natural gas consumption of 18,687—22,357 CFH.

The technology demonstrated under this project requires only 6.7 MMBtu/hr (7,000—8,000 CFH) of heat for optimal ejector network operation. Due to the heat pumping arrangement of energy transformation, such a thermal input is sufficient to generate and sustain a dynamic vacuum at the designed level, as well as for heating the drying

product to the designed temperature. Therefore, the thermo-vacuum system has a strong potential to reduce gas consumption by 61—65 percent for the same drying product throughput.

As to primary energy consumption, the demonstrated thermo-vacuum system differs from the state-of-the-art equipment by mostly pumping power that was 8-10 kW, while the off-shelf drying equipment requires 5-6 kW recirculating pumps and over 20kW to power the air fans. Thus, the thermo-vacuum system demonstrated an obvious reduction in primary energy consumption by at least 40 percent.

5.2 Impacts and Benefits to California Ratepayers

The results of the demonstration do show the potential of the system to evacuate moisture with simultaneous product heating and heat pumping effect. With further refined engineering and smart automation, the system can progress toward commercialization. At the same time, the results revealed the potential to consider another type of boiler, and identified the necessary upgrades and the design adjustments of the holo-flite and its supporting units.

Successful implementation of demonstrated gas-fired thermo-vacuum dryer technology with advanced heat pump system integration throughout the qualified California food processing applications offers a path toward significant energy savings within the state's industrial market. The technology concept can also be adapted to other drying and food processing applications besides the screw-type dryer specifically used in this demonstration. Application across a broad range of technologies will result in end-user fuel savings (over 60 percent), reduced pollutant emissions (at least 10 percent), and the potential for moisture recovery and reuse.

The research team estimates that an electric heat pump with an assumed coefficient of performance (COP) of 6, and an ejector-based heat pump with a projected COP of 2, could result in cost savings of 6 percent and 63 percent, respectively, when compared to direct fired gas drying.

The heat pumping integration into the thermos-vacuum drying system significantly enhances its performance efficiency, economics, and reduction of greenhouse gas emissions.

The expected environmental benefits are significant. The higher efficiency compared with traditional rotary dryers ensures a favorable environmental impact because the integrated thermo-vacuum system provides the end-user with fuel savings, resulting in fewer products of combustion, including carbon dioxide and other pollutants as estimated above. Moisture recovery from the system exhaust can provide additional benefits to end-users in the form of complementary hot water services, irrigation, etc.

Table 8: Specific Performance of Heat Pumping Over Direct Gas-Fired Drying

Heat Source	Output Energy Required (MWh)	COP	Input Energy Required (MWh)	Energy Rate ($/kWh)	Annual Energy Cost	Cost Savings vs. Direct Fired	% Savings	Cost of Heat Pump	Payout in Years
Direct Fired Gas	1	0.75	1.33	$0.0145	$162,400				
Electric HP	1	6.00	0.17	$0.1095	$153,300	$9,100	6%	$400,000	43.96
Ejector HP	1	2.00	0.50	$0.0145	$60,900	$101,500	63%	$400,000	3.94

****Based on industrial natural gas and electricity rates in California and annual operations of 350 days/year**

Source: GTI

The indirect gas-fired drying market accounts for about 5 percent of the total natural gas consumption across the commercial and industrial sectors. Per USEIA, about 10 TCF of natural gas was consumed in 2012 by commercial and industrial customers nationwide, and indirect drying operations consumed about 0.5 TCF. At average energy efficiency of the typical dryers (~35—40 percent), the wasted energy from drying processes can be estimated at 300 quads. Applying the thermos-vacuum technology (with at least 75 percent energy efficiency) to 100 percent of the commercial and industrial gas-fired drying processes would provide energy savings of approximately 60 percent, or about 0.3 TCF, as opposed to conventional operations. In California, dried and dehydrated fruits and vegetables processing was estimated in 2005 to consume over 6.2 TBtu per year (Report No. GRI-03/0075). Considering market growth over the last decade, and assuming a natural gas price of at least $5.00 per MMBtu, the demonstrated thermos-vacuum drying technology has the potential to save $20 million and 200 tons of CO_2 per year statewide in agricultural drying operations alone.

5.3 Recommendations

Detailed simulation of the ejector system and dryer process flow and prototype laboratory evaluation indicated the potential for significant energy savings through the use of an ejector-based thermo-vacuum heat pump drying system.

Evaluation of the installed thermo-vacuum drying system at the participating food processing site clearly demonstrated the high level and quality of the calculation, design, and manufacturing of the ejectors, which consistently produced the calculated parameters and automatically shifted to the designed limit load corresponding to the lower suction pressure. The condensing steam after ejectors effectively heats up the product transporting by and along the heated flites in the drying volume that is under dynamic vacuum condition. The combination of product heating and volume vacuuming is a core of the demonstrated technology, and results in significant energy and cost benefits.

Preliminary cost estimates indicated a capital cost reduction in at least in two times taking into account the adequate replacement of the recirculation pumps and air fans with the ejectors and heat exchangers.

The following steps to move the demonstrated technology forward are recommended for the pre-commercial engineering phase:

- Product charge and discharge systems and integration into the main control scheme should be optimized.
- The optimal mesh size of the return condensate filter should be determined and outsourced.
- An alternative boiler system for outdoor applications should be identified.
- The steam is currently vented to the atmosphere. The follow-on engineering design should require a steam-condensing unit to harvest excess water with

minimal product residue that can be used for irrigation, cooling, or other purposes.

- The low-grade process heat unutilized in technology can be converted into electricity via an Organic Rankine cycle, if needed for internal use by the drying operator or to be sold to the local grid.
- To further improve the efficiency of drying performance, it is recommended to utilize the excess heat from steam condensation after ejectors was not included in the scope of this technology demonstration project.

REFERENCES

[1] D. M. Parikh, "Solids Drying: Basics and Applications," Chemical Engineering: Essentials for the CPI Professional, 2014. [Online]. Available: https://www.chemengonline.com/solids-drying-basics-and-applications/?pagenum=1. [Accessed: 24-Jan-2019].

[2] "Direct-Fired vs. Indirect-Fired Rotary Dryers," Applied Chemical Technology, 2019. [Online]. Available: https://appliedchemical.com/equipment/rotary-drums/directly-heated-vs-indirectly-heated-rotary-dryers/. [Accessed: 07-Feb-2019].

[3] The Witte Company Inc., "Fluid Bed Dryer," 2015. [Online]. Available: http://www.witte.com/product/fluid-bed-dryer/. [Accessed: 15-Jan-2019].

[4] Y. Chudnovsky, "High Efficiency Gas-Fired Drum Dryer for Food Processing Applications." California Energy Commission, PIER Industrial/Agricultural/Water End-Use Energy Efficiency Program, 2011.

LIST OF ACRONYMS

Term	Definition
AHP	Advanced heat pump
Anergy	Dilute or disorganized energy which cannot be converted to work
BFE	Binary fluid ejector
BHP	Brake horsepower
Btu	British thermal unit
CFD	Computational fluid dynamics
CFH	CFH
CO	Carbon monoxide
CO2	Carbon dioxide
COP	Coefficient of performance
GFDD	Gas-fired drum dryer/drying
GFTD	Gas-fired thermal-vacuum dryer/drying
GHG	Greenhouse gas(es)
GWP	Global Warming Potential
GTI	Gas Technology Institute
H2	Hydrogen
Hz	Hertz
HP	Heat pump
IAW	Industrial, Agricultural, and Water (California Energy Commission Energy Efficiency Program)
IEF	Inland Empire Foods
IGFRD	Indirect gas-fired rotary dryer
kPa	KiloPascal
MMBtu	Million Btu
M&V	Measurement and verification
NOx	Nitrogen oxides

Term	Definition
ODP	Ozone Depletion Potnetial
PI&D	Process and instrumentation diagram
Psi	Pounds per square inch
RH	Relative Humidity
SCAQMD	South Coast Air Quality Management District
TBtu	Trillion Btu
TCF	Trillion cubic feet
TDES	Thermal-driven ejector system
TDR	Thermally-driven refrigeration
TVDS	Thermo-vacuum drying system
USEIA	United States Energy Information Administration

APPENDIX A:
System Assembly and P&IDs

This Appendix contains system diagram layouts and P&IDs of the Thermovacuum Ejector-Based Drying System installed at Martin Feed LLC.

Whole System Layouts

Figure A-1: Overview of Thermovacuum Assembly

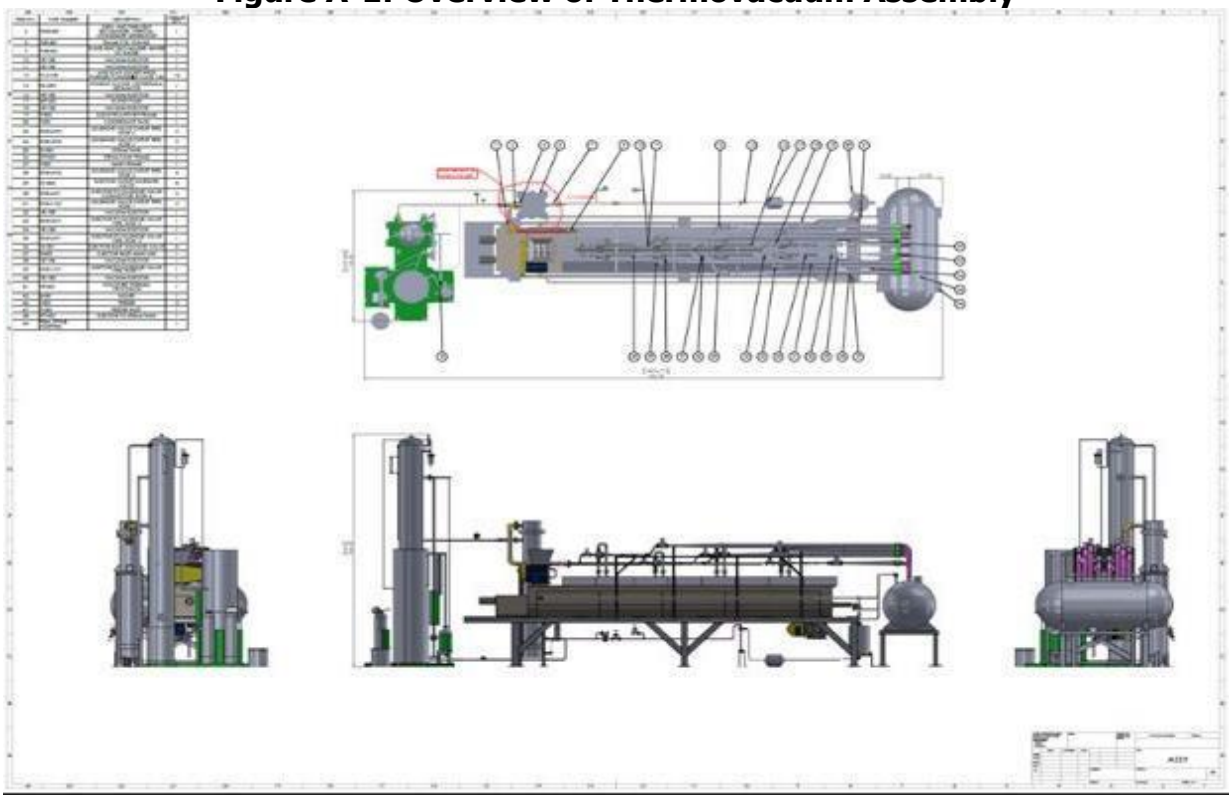

Source: GTI

Figure A-2: Thermovacuum System Assembly (Top View)

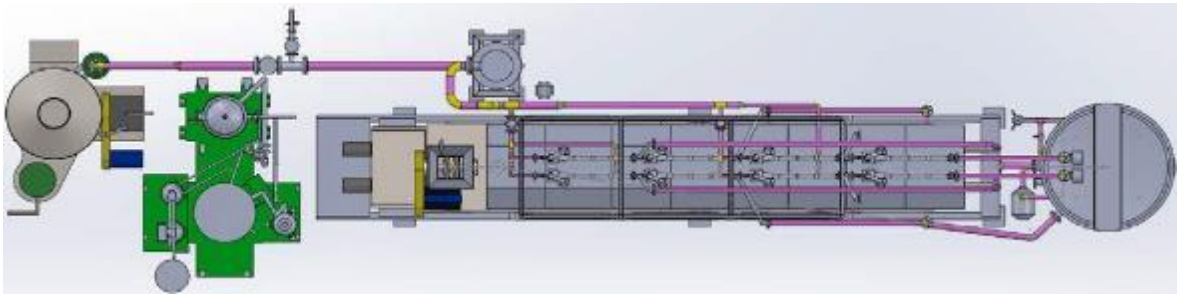

Source: GTI

Figure A-3: Holo-flite® and Ejector Parts Assembly

Source: GTI

Figure A-4: Isometric View of Holo-flite®

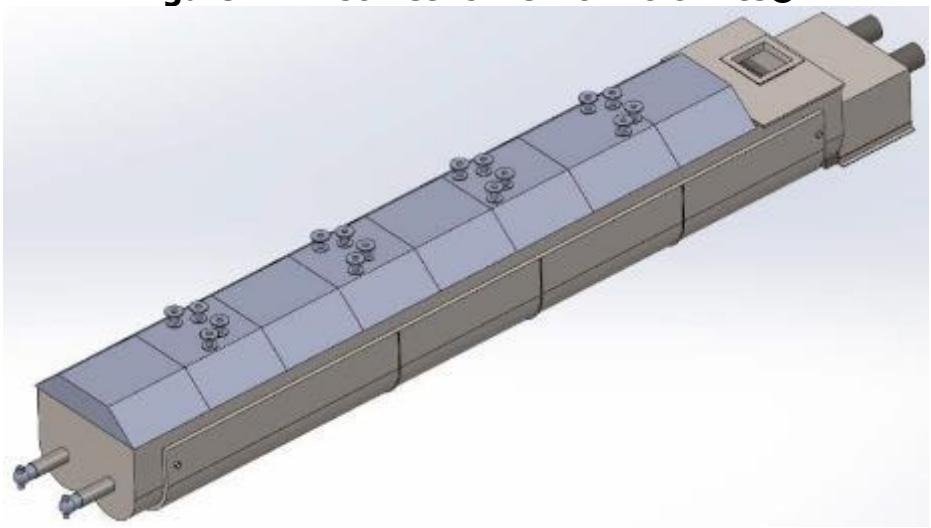

Source: GTI

Figure A-5: Boiler and Condensate Tank

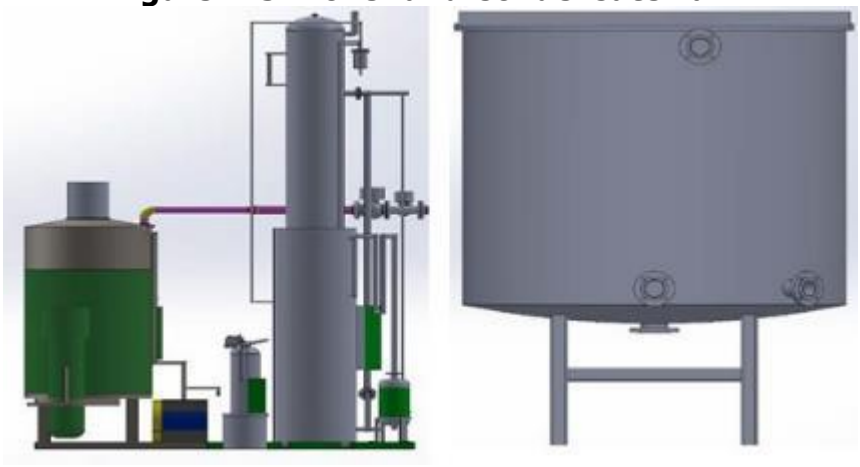

Source: GTI

Ejector Layouts

Figure A-6: Ejector

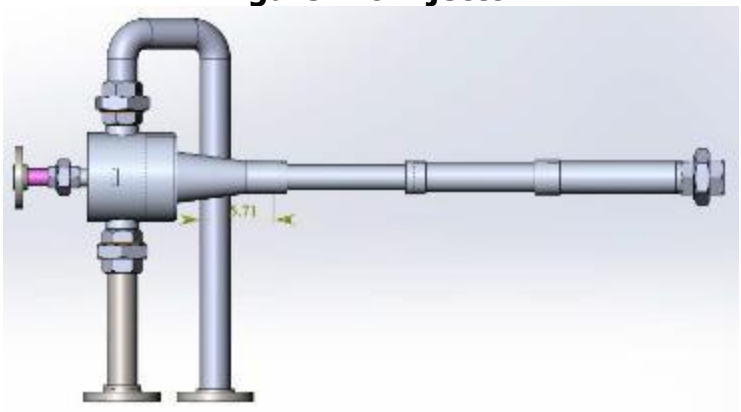

Source: GTI

Figure A-7: Ejectors (Side and Top Views)

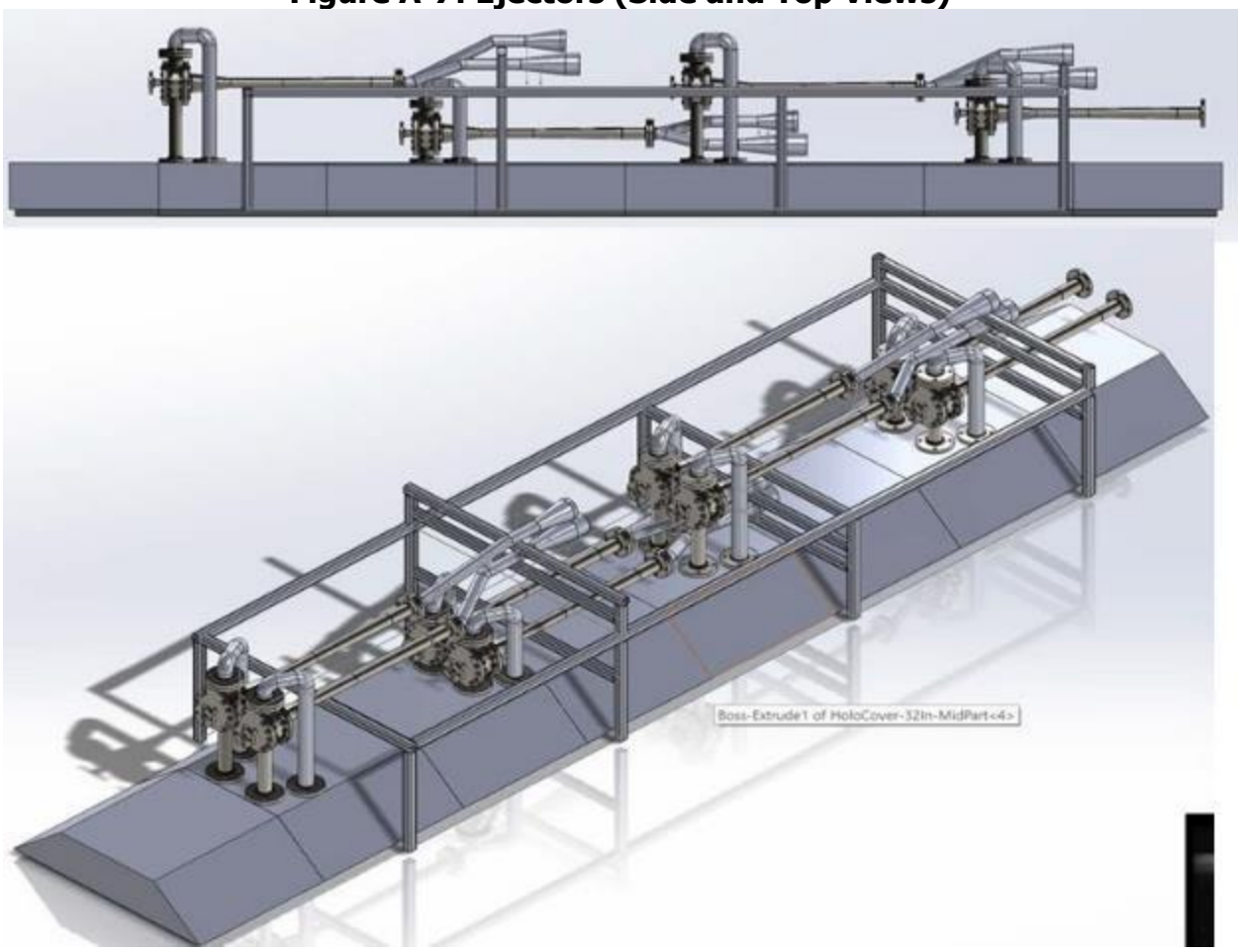

Source: GTI

APPENDIX B:
System Design and Specification Package

This Appendix covers some of the detailed calculations associated with the design of the ejectors and advanced drying system.

3D-Modeling of Ejector

The 3 dimensional model of the ejector was performed using CFD software and in house code for geometry profile optimization and entrainment ratio calculations.

CFD Modeling: Order of Construction

1. A preliminary calculation of the geometrical parameters of the flow part of the ejector is performed using a universal program.

2. The obtained geometric characteristics serve as the basis for building an ejector in the editor.

3. On the basis of the equations of the mathematical model of the ejector, the number of dimensions of the flow part of the ejector is refined, which are not uniquely determined.

4. The construction of the computational grid based on the finite element method. In order to maximize the concentration of grid cells on the model, only a quarter of the ejector consisting of 5082201 elements was used in the calculation process, which does not affect the quality of the results obtained.

5. The flow-through part of the ejector with its shape and dimensions obtained by modeling is transferred to an electronic drawing that is used directly in the manufacture of the ejector. As a result, the resulting real ejector has the highest energy performance possible.

Mathematical Model of the Ejector: Basic Equations

The continuity equation

$$\frac{\partial \rho}{\partial t} + \nabla \cdot (\rho U) \quad 0 \qquad \text{(A.1)}$$

where ρ – density (ML^{-3}), t – time (T), U – velocity (LT^{-1}).

The equation of conservation of momentum

$$\frac{\partial (\rho U)}{\partial t} + \nabla \cdot (\rho U \otimes U) \quad -\nabla p + \nabla \cdot \tau + S_M \qquad \text{(A.2)}$$

$$\tau - \mu \left(\nabla U - (\nabla U)^T - \frac{2}{3} \delta \nabla \cdot U \right) \qquad \text{(A.3)}$$

where τ stress tensor ($ML^{-1}T^{-2}$), S_M – pulse source ($ML^{-2}T^{-2}$), δ Kronecker delta unit matrix, T – static temperature (Θ)

The equation of total energy

$$\frac{\partial(\rho h_{полн})}{\partial t} - \frac{\partial p}{\partial t} + \nabla \cdot (\rho U h_{полн}) = \nabla \cdot (\lambda \nabla T) + \nabla \cdot (U \cdot \tau) + U \cdot S_u + S_E \qquad (A.4)$$

$$h_{полн} = h + \frac{1}{2}U^2 \qquad (A.4.1)$$

where $h_{полн}$ total enthalpy depending on static enthalpy $h(T, p)$, S_E energy source ($ML \cdot T^{-3}$), λ thermal conductivity ($MLT^{-3}\Theta^{-1}$), $\nabla \cdot (U \cdot \tau)$ - friction work, describes work related to viscous stress, $U \cdot S_u$ - work under the influence of external sources (neglected in this case).

Mathematical Model of Turbulence

Two-parameter turbulence models are widely used because they offer a good compromise between numerical achievements and computational accuracy. Although at the same time, the two-parameter model is much more complicated than the "non-parametric" (zeroequation) model, since it considers speed and linear lengths in various transport equations.

The k - ε and k - ω models use the parameter gradient diffusion hypothesis to relate the Reynolds stresses with average velocity and turbulent viscosity. Turbulent viscosity is determined from turbulent velocity and linear length.

In the models of two equations, the velocity values are calculated from the kinetic energy of the turbulent flow obtained by solving the transport equation. The turbulent length is determined from 2 properties of the turbulence field, the kinetic energy of the turbulent flow, and the intensity of its dispersion. The intensity of dispersion is also determined from the solution of the transport equation.

k-ω Model

One of the advantages of the k-ω model is the consideration in the calculations of low-rinsing flows in the surface layer. The model does not involve the use of complex non-linear functions required for the k-ε model, which gives a more accurate and reliable result. The low-root k-ε model typically requires y - ≈0.2 while k-ω requires y - ≈2. However, in industrial currents, even y - <2 cannot be guaranteed in most applications, therefore, a new method for calculating the parameters of the surface layer was developed for the k-ω model. It allows you to more smoothly make the transition from the low-rhythm flow model to the near-wall functions. Let us briefly consider some new models for calculating the parameters of the surface layer with a transition to a turbulent flow.

The k-ω model assumes that the viscosity of a turbulent flow is related to kinetic energy and friction in a turbulent flow:

$$\mu_t = \rho \frac{k}{\omega} \qquad (A.5)$$

where μ_t - turbulent viscosity ($ML^{-1}T^{-1}$), ρ - density (ML^{-3}), ω - angular velocity (T^{-1}).

k-ω Wilcox Model

This model solves 2 transport equations: the kinetic energy equation of the turbulent flow k (A.6) and the friction in the turbulent flow ω (A.7). The stress tensor is calculated from the viscosity of the turbulent flow.

$$\frac{\partial(\rho k)}{\partial t} \quad \nabla\cdot(\rho \boldsymbol{U} k) = \nabla\left[\left(\mu + \frac{\mu_t}{\sigma_k}\right)\nabla k\right] \quad P_k \quad P_{kb} \quad \beta'\rho k\omega \qquad (A.6)$$

$$\frac{\partial(\rho\omega)}{\partial t} + \nabla\cdot(\rho \boldsymbol{U}\omega) = \nabla\left[\left(\mu + \frac{\mu_t}{\sigma_\omega}\right)\nabla\omega\right] + \alpha\frac{\omega}{k}P_k + P_{\omega b} - \beta'\rho\omega^2 \qquad (A.7)$$

where

$$\beta' = 0.09$$

$$\alpha = 5/9$$

$$\beta = 0.075$$

$$\sigma_k = 2$$

$$\sigma_\omega = 2$$

where k – turbulence kinetic energy per unit mass (L^2T^{-2}), μ – molecular (dynamic) viscosity ($ML^{-1}T^{-1}$), μ_t – turbulent viscosity ($ML^{-1}T^{-1}$), P_k – turbulence kinetic energy production ($ML^{-1}T^{-3}$), P_{kb} – производство выталкивающей силы, ω – угловая скорость (T^{-1}), $\boldsymbol{U}$ – speed vector (LT^{-1}), $P_{\omega b}$ – extra buoyant member for k-ω model.

Unknown stress tensor $\rho\overline{\boldsymbol{u}\otimes\boldsymbol{u}}$ is defined from:

$$-\rho\overline{\boldsymbol{u}\otimes\boldsymbol{u}} = \mu_t\left(\nabla U + (\nabla U)^T\right) - \frac{2}{3}\delta\left(\rho k + \mu_t\nabla\cdot U\right) \qquad (A.8)$$

where $\boldsymbol{u}$– fluctuating velocity component in a turbulent flow (LT^{-1}), T – statis temperature (Θ),

In addition to the independent variables, the density ρ and the velocity vector U are treated as known values of the Navier-Stokes equation. P_k is the derived turbulence value obtained from the following equation 25 of the k-ε model:

$$P_k = \mu_t\nabla\boldsymbol{U}\cdot\left(\nabla U + \nabla\boldsymbol{U}^T\right) - \frac{2}{3}\nabla\cdot\boldsymbol{U}\left(3\mu_t\nabla\cdot\boldsymbol{U} + \rho k\right) \qquad (A.9)$$

For incompressible flows ∇·U has a small value and the second term of the right side of the equation does not make a significant contribution. For a compressible flow ∇·U has large values in areas with a large divergence of speed, such as shocks.

If P_{kb} takes positive values, then the definition of pushing force is included in the equation for determining k, if its calculation function is included in CFX. For its definition are used (2.53) or (2.54):

$$P_{kb} = -\frac{\mu_t}{\rho\sigma_\rho} g \cdot \nabla\rho \qquad (A.10)$$

$$P_{kb} = \frac{\mu_t}{\rho\sigma_\rho} \rho\beta g \cdot \nabla T \qquad (A.11)$$

where β– gravity vector (LT^{-2}).

It is also included in the equation ω, if the corresponding option is enabled.

$$P_{\omega b} = \frac{\omega}{k}\left((\alpha - 1)C_3 \max\left(P_{kb}, 0\right) - P_{kb}\right) \qquad (A.12)$$

where C= 1 - dissipation vector.

If the option of taking into account the direction of flows is enabled, then equation (A.55) takes the following form:

$$P_{\omega b} = \frac{\omega}{k}\left((\alpha + 1)C_3 \max\left(P_{kb}, 0\right) \cdot \sin\phi - P_{kb}\right) \qquad (A.13)$$

where ϕ - angle between speed and gravity vector.

Baseline k-ω (BSL k-ω).

The main problem of the Wilcox model (A.57, A.58) is high dependence on the state of free flow. Depending on the set value ω for the input stream, there is a significant difference in the results obtained. To solve this problem, Menter (9) proposed to combine 2 models: k ω for the solution in the near-wall region and modified k-ε (A.59, A.60) - away from the near-wall region. Also added the corresponding equations of transition from one model to another. Thus, the Wilcox mathematical model is multiplied by the function F_1, and the k ε model is changed by the function 1-F_1. On the border of the boundary layer and outside it, the standard k-ε model is used.

Wilcox model:

$$\frac{\partial(\rho k)}{\partial t} + \nabla \cdot (\rho U k) - \nabla \cdot \left[\left(\mu + \frac{\mu_t}{\sigma_{k1}}\right)\nabla k\right] + P_k - \beta' \rho k\omega \qquad (A.14)$$

$$\frac{\partial(\rho\omega)}{\partial t} + \nabla \cdot (\rho U\omega) = \nabla \cdot \left[\left(\mu + \frac{\mu_t}{\sigma_{\omega 1}}\right)\nabla\omega\right] - \alpha_1 \frac{\omega}{k} P_k - \beta \rho k\omega^2 \qquad (A.15)$$

where

$$\beta' - 0.09$$

$$\alpha_1 = 5/9$$

$$\beta_1 = 0.075$$

$$\sigma_{k1} = 2$$

$$\sigma_{\omega 1} = 2$$

Modified $k\varepsilon$ model:

$$\frac{\partial(\rho k)}{\partial t} + \nabla \cdot (\rho \mathbf{U} k) = \nabla \cdot \left[\left(\mu - \frac{\mu_t}{\sigma_{k2}} \right) \nabla k \right] + P_k - \beta' \rho \mathbf{k} \omega \qquad \text{(A.16)}$$

$$\frac{\partial(\rho\omega)}{\partial t} + \nabla \cdot (\rho \mathbf{U} \omega) - \left(\nabla \cdot \left[\left(\mu + \frac{\mu_t}{\sigma_{\omega 2}} \right) \nabla \omega \right] \right) + 2\rho \frac{1}{\sigma_{\omega 2} \omega} \nabla k \nabla \omega + \alpha_2 \frac{\omega}{k} P_k - \beta_2 \rho k \omega^2$$

(A.60)

where

$$\alpha_2 = 0.44$$

$$\beta_2 = 0.0828$$

$$\sigma_{k2} = 2$$

$$\sigma_{\omega 2} - 2$$

Now, the equations of the Wilcox mathematical model are multiplied by F_1, the modified equations of the k-ε model are 1-F_1, and the corresponding equations for k and ω are added to formulate the BSL model. Thus, taking into account the effect of lift, the BSL model takes the form:

$$\frac{\partial(\rho k)}{\partial t} + \nabla(\rho \mathbf{U} k) - \nabla \cdot \left[\left(\mu + \frac{\mu_t}{\sigma_{k\omega}} \right) \nabla k \right] - P_k - P_{kb} - \beta' \rho k \omega \qquad \text{(A.17)}$$

$$\frac{\partial(\rho\omega)}{\partial t} - \nabla \cdot (\rho \mathbf{U} \omega) = \nabla \cdot \left[\left(\mu - \frac{\mu_t}{\sigma_{\omega\omega}} \right) \nabla \omega \right] + (1 \quad F_1) 2\rho \frac{1}{\sigma_{\omega 2} \omega} \nabla k \nabla \omega + \qquad \text{(A.18)}$$

$$-\alpha_3 \frac{\omega}{k} P_k + P_{\omega b} - \beta_3 \rho k \omega^2$$

The coefficient α in the equations for determining $P_{\omega b}$ in equations 12 and 13 is replaced by α3. Model coefficients are a linear combination of the corresponding base model coefficients.

$$\Phi_3 = F_1\Phi_1 + (1 - F_1)\Phi_2 \quad (A.19)$$

where Φ_1 – represents all the constants from the original model, Φ_2 – represents constants from a modified model $k\varepsilon$. Φ_3 new model coefficients.

Shear Stress Transport (SST)

The turbulence model SST (Shear Stress Transport) is based on the k-ω model for the distribution of turbulent stress and provides more accurate predictions of the onset of separation and flow rate with adverse pressure drops.

The BSL model combines the benefits of the k-ε and Wilcox models. However, it still does not allow to determine the beginning of the flow separation from the smooth surface. The main reason for this is that both models do not take into account the turbulent stress in the transport equation. This results in overestimated viscosity values of the swirling flow. The correct transport equation can be obtained by introducing a constraint to determine the turbulent viscosity:

$$\upsilon_t \quad \frac{a_1 k}{\max(a_1\omega, SF_2)} \quad (A.20)$$

$$\upsilon_t = \mu_t / \rho \quad (A.21)$$

Where S absolute value of turbulence, F_2 equal to 1 for flows in the border layers or 0 for free layers.

Also F_1 is a n interface function similar to F_1, which imposes restrictions on (A.64) for the near-wall layer, and the underlying assumptions are not true for free vortex flows. S - invariant measure of propagation velocity.

Interface functions are important for this method and depend on the distance to the nearest surface and the flow variables.

$$F_1 = tahn\left(\arg_1^4\right) \quad (A.22)$$

where

$$\arg_1 = \min\left(\max\left(\frac{\sqrt{k}}{\beta'\omega y}, \frac{500\upsilon}{y^2\omega}\right), \frac{4\rho k}{CD_{k\omega}\sigma_{\omega 2} y^2}\right) \quad (A.23)$$

where y – distance to the nearest wall, ν kinematic viscosity and

$$CD_{k\omega} = \max\left(2\rho \frac{1}{\sigma_{\omega 2}\omega} \nabla k \nabla \omega, 1.0 \times 10^{-10}\right) \quad (A.24)$$

$$F_2 = tahn\left(\arg_2^2\right) \tag{A.25}$$

$$\arg_2 = \max\left(\frac{2\sqrt{k}}{\beta'\omega y}, \frac{500\upsilon}{y^2\omega}\right) \tag{A.26}$$

where F_2 is equal to 0, if $y^2>70$.

Algorithm for constructing a mesh and setting boundary conditions

The construction of the computational mesh to optimize the flow part of the ejector is as follows:

For CFD modeling, a tetrahedral mesh with prismatic elements was used, with the following parameters:

1. Physics preference – CFD
2. Mesh method – Patch Independent
3. Use Advanced Size function - On: Proximity and Curvature.
4. Relevance center – Fine
5. Smoothing - high
6. Transition – Slow
7. Curvaturenormalangle - 10°
8. Minsize – 0.135 mm
9. Growth rate – 1.2
10. Automatic Inflation – Program Controlled
11. Inflation Option – First Layer Thickness
12. First Layer Height - 0.05 mm
13. Maximum Layers - 15
14. Growth Rate – 1.2
15. Inflation Algorithm – Pre
16. Collision Avoidance – Stair Stepping
17. Gap Factor – 0.5
18. Maximum Height over Base - 0.1
19. Growth Rate – Geometric
20. Maximum Angle – 180°C
21. Fillet Ratio – 1
22. Use Post Smoothing - Yes, Smoothing Iterations - 10.
23. Shape Checking – CFD

Using BodySizing for the receiving chamber, where there is acceleration of the ejected flow and acceleration of the working flow in the diffuser part of the nozzle, as well as the mixing chamber, where compression shocks are observed, the dimensions of the mesh elements are different from the basic dimensions indicated above.

Inflation was made for two areas: nozzle walls and walls of suction chamber, mixing chamber and diffuser (Fig. A.1) .

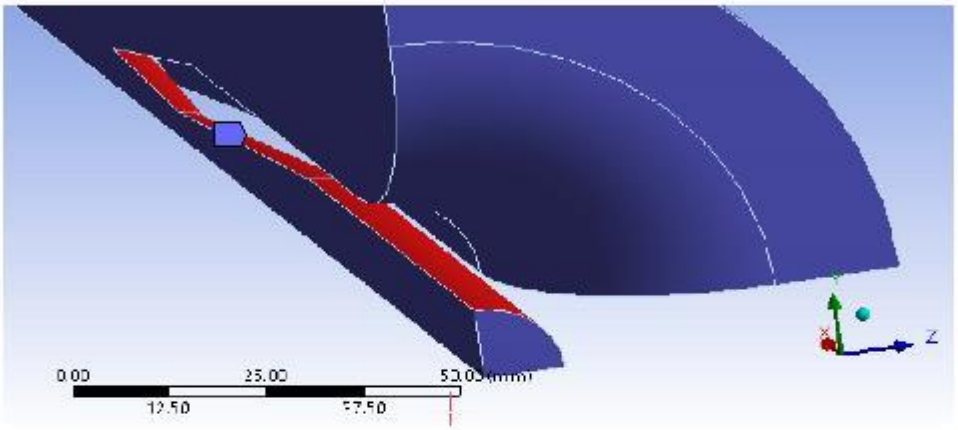

A) Inflation area of nozzle.

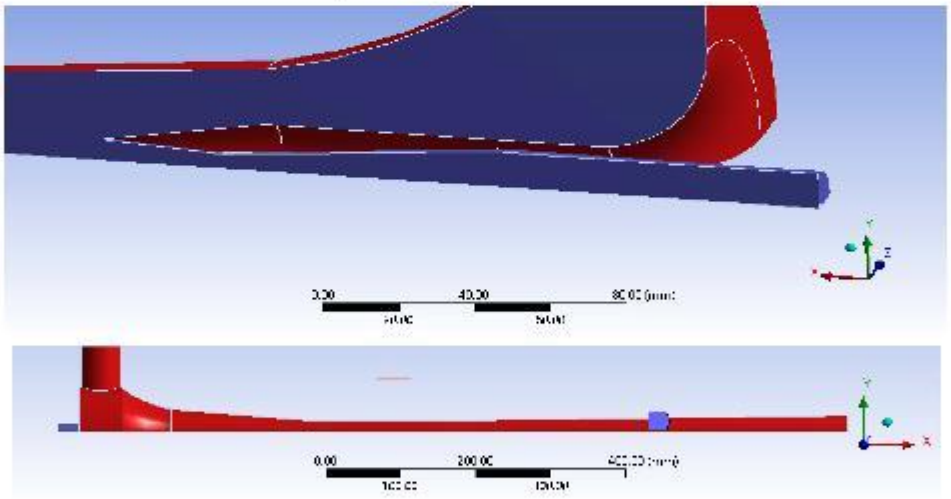

B) Inflation area of suction chamber, mixing chamber and diffuser.

Fig. B-1. Inflation areas

For the wall separating the ejected and the working flow at the nozzle exit, Face Sizing with Element sizing is set to 0.03 (Figure B.2)

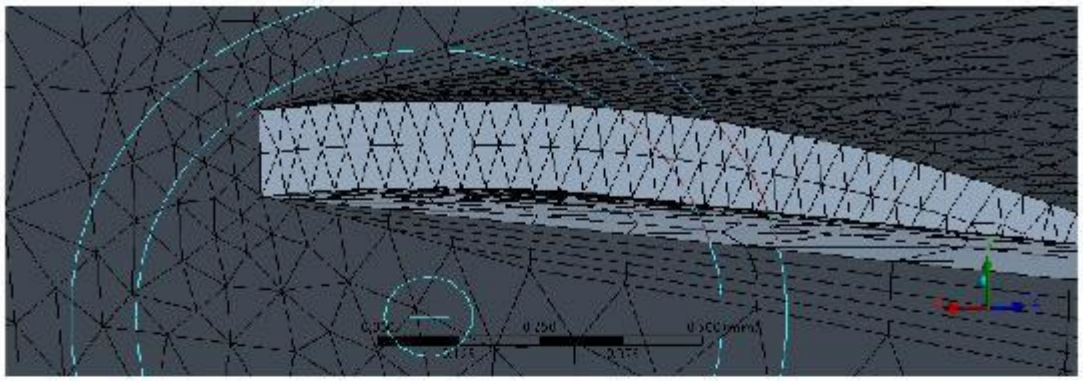

Fig. B.2 Area of local mesh resizing.

The result of the mesh (Fig. B.3): the number of points - 1178628, elements - 5082201. The minimum Aspect Ratio value is 1.16, the maximum is 40, the average is 3.6. The values of Skewness lie in the range of 0.002 - 0.56, the average value is 0.18.

A) Critical and output nozzle section, receiving chamber.

Б) Cylinder mixing chamber

В) Diffuser

Fig. B.3 Calculated mesh

Modelling parameters

DomainBoundaryConditions.

Basic Settings.

Domain Type - Fluid Domain

Material - Material Library - H_2O-Air

Morphology Option Continuous Fluid.

Reference pressure 0 [Pa]

Buoyancy Model Non Buoyant

Domain Motion - Stationary

Fluid Models.

Heat Transfer - Total Energy

Turbulence - Option - Shear Stress Transport

Wall Function - Automatic

Initialization

Cartesian Velocity Components Automatic.

Velocity Scale 2.5 m/s

Static Pressure Automatic with Value

Relative Pressure - 70000 [Pa]

Temperature - Automatic with Value

Temperature - 90 [C]

Turbulence - Option - Medium (Intensity = 5%)

Boundary Details.

Mass and Momentum - No Slip Wall

Wall Roughness - Option - Smooth Wall

Heat Transfer - Option - Adiabatic

Working Flow Boundary Conditions

Boundary Type Inlet

Flow Regime - Subsonic

Mass and Momentum - Static Pressure

Relative Pressure - 792190 [Pa]

Flow Direction - Zero Gradient

Turbulence - Zero Gradient

Heat Transfer - Static Temperature

Static Temperature 171 [C]

Ejected Flow Boundary Conditions

Boundary Type - Inlet

Flow Regime - Subsonic

Mass and Momentum - Static Pressure

Relative Pressure - 70000 [Pa]

Flow Direction - Zero Gradient

Turbulence - Zero Gradient

Heat Transfer Static Temperature

Static Temperature 90 [C]

Outlet Flow Boundary Conditions

Boundary Type - Outlet

Flow Regime - Subsonic

Mass and Momentum - Static Pressure

Relative Pressure - 101325 [Pa]

Solver Control Parameters

Advection Scheme - High Resolution

Turbulence Numerics First Order

Physical Time Scale 4e-005 [s]

Residual Type - RMS

Residual Target - 1e-05

Conservation Target - 0.005

Advanced Options

Global Dynamic Model Control - checked

Compressibility Control - checked

High Speed Numerics - checked

Total Pressure Option Automatic

Material - H_2O

Basic Settings

Option - Pure Substance

Thermodynamic State - Gas

Material Properties

Option - General Material

Thermodynamic properties

Equation of State

Option Real Gas

Model Peng Robinson

Molar Mass - 18.015 [kg/kmol]

Critical Temperature - 647.14 [K]

Critical Pressure - 220.64 [Bar]

Critical Volume - 55.95 [cm /mol]

Acentric Factor - 0.334

Boiling Temperature - 373.15 [K]

Specific Heat Capacity

Option Real Gas

Zero Pressure Coefficients Fourth Order Polynomial

A1 4.395

A2 = -4.186e-3 [1/K]

A3 = 1.405e-5 [1/K^2]

A4 = -1.564e-8 [1/K^3]

A5 = 0.632-11 [1/K⁴]

Low Cp0(T) Temperature Limit = 100 [K]

Upper Cp0(T) Temperature Limit = 1000 [K]

Reference State

Option Automatic

Table Generation

Minimum Temperature = 100 [K]

Maximum Temperature = 1000 [K]

Minimum Absolute Pressure = 1000 [Pa]

Maximum Absolute Pressure = 1e+06 [Pa]

Transport Properties

Dynamic Viscosity

Option = Kinetic Theory Model

Option = Interacting Sphere

Thermal Conductivity

Option = Kinetic Theory Model

Option = Modified Eucken

Material = Air

Basic Settings

Option = Pure Substance

Thermodynamic State = Gas

Material Properties

Option = General Material

Thermodynamic properties

Equation of State

Option =Value

Molar Mass = 28.96 [kg/kmol]

Density = 1.185 [kg/m³]

Specific Heat Capacity

Option - Value

Specific heat capacity - 1.0041e+03 [J/(kg K)]

Specific heat type - Constant pressure

Reference State

Option Specific point

Ref. Temperature 25 [C]

Reference pressure 1 [atm]

Transport Properties

Dynamic Viscosity

Option - Value

Dynamic Viscosity - 1.831e-05 [kg/(m s)]

Thermal Conductivity

Option - Value

Thermal Conductivity 2.61e-02 [W/(m K)]

Efficiency of Ejector Heat Pump vs. Vapor Compression Heat Pump

Generally speaking, the process in a heat pump can be reduced to the fact that some exergy is added to the anergy, which results in heat that can be transferred to a heated object at a higher temperature, i.e. produce a heating effect. In our case, instead of anergy, we use the enthalpy of the flow, which has thermal disequilibrium with the environment and add to it the kinetic energy of the flow with greater exergy, obtained by converting energy from pressure. Thus, the amount of high-temperature heat is equal to the full amount of heat of combustion of the fuel. In the vapor compression cycle of a compressor-driven heat pump, only part of the heat of combustion of the fuel is used: heat of combustion is converted into work (electricity), taking into account losses during its transfer and conversion of voltage from low to high, and then lowering the voltage at the consumer. As a result, the efficiency of the jet heat pump is 1.4-2 times higher. Indeed, the efficiency of the heat pump based on the heat input on the power plant can be calculated as follows:

$$\varphi = \frac{Q_{низ} + L}{Q_{вих}} \qquad (2.27)$$

where $Q_{низ}$- heat removed from a low exergy source

L the work cycle of the heat pump, equal to the work expended on the compressor drive.

$Q_{вих}$ heat expended in power generation at power plants

The work expended on the compressor drive is equal to

$$L \quad Q_{gen}\eta_e\eta_h \tag{2.27}$$

where: η_e=0,3-0,4 – efficiency of real power cycle, η_h – energy transfer efficiency at utilities.

Then

$$\varphi = \left(Q_{evap} + Q_{gen}\eta_e\eta_{tr}\right) / Q_{gen} = Q_{evap} / Q_{gen} + \eta_e\eta_{tr} \tag{2.28}$$

$$Q_{evap} = L\varepsilon \tag{2.29}$$

where ε -cooling capacity, (equal to 3-4 for the parameters discussed).

When electricity is transmitted from the generator to the consumer, usually up to 10% of the primary energy is lost, i.e. η_h=0,9. Then

$$L = \left[0.3 : 0.4\right] \times 0.9 \times Q_{gen} = \left[0.27 : 0.36\right] \times Q_{gen} \tag{2.30}$$

In this case, the conversion factor of the heat pump will have the following range of values

$$\varphi = \varepsilon\left[0.27 - 0.36\right] + \left[0.27 - 0.36\right] \tag{2.31}$$

At ε=3 φ= 1,08 – 1,44

At ε = 4 φ= 1,35 – 1,8

For the ejector heat pump:

$$\varphi = \left(Q_{evap} + Q_{gen}\right) / Q_{gen} = 1 + Q_{evap} / Q_{gen} = \zeta + 1 \tag{2.32}$$

where ζ – thermal coefficient. In considered modes ζ = 1 for single fluid heat pump, and for binary fluid - ζ= 1.5 and more. Thus, the values of the conversion coefficient change from 2 to 2.5.

This means that the real efficiency of the jet heat pump is 1.4-1.8 times higher than that of the traditional one. In addition, the jet heat pump has a large temperature range for its work.

Ejector Operation Principles

Despite the simplicity of the device and the simple principle of operation of the ejector, which was mentioned earlier, the nature of the processes occurring in the ejector has not yet been fully investigated and ambiguous. The complex hydrodynamic model of the flow, as well as the interaction of flows with significantly different initial velocities, inelastic shock, shock waves, shock waves, makes the picture of the work of the ejector very complex, which is almost impossible to describe analytically. Of particular difficulty is the work of the ejector in off-design conditions, which almost always arise in practice, since strictly maintaining a stable set of operating parameters is simply not possible. First of all, it concerns the environmental parameters, which vary regardless of the technological process.

In the process of the ejector, a number of inevitable losses arise. The greatest of these are the losses due to the collision of the active and passive jets in the receiving chamber. These losses are proportional to the square of the difference in the velocity of the moving flows. In this case,

The active flow has a speed, as a rule, 1.5-2 times the speed of sound, and the ejected flow has a speed approximately in the region of 0.5-0.6 of the speed of sound. As practice shows, the magnitude of these losses lies within 30-60% of the total energy balance of the ejector. (ejector circuit)

As follows from the picture of outflow of flows, there is no complete physical mixing of flows in the flow part of the ejector; it is inherent only in a small boundary zone, which increases as it approaches the exit from the diffuser. Impulse transfer occurs with a more or less elastic collision, which suggests this process is more reversible than a completely inelastic impact. In addition, a direct shock wave does not entail complete mixing, which also slightly reduces additional losses. We can confidently state that the core of the cross section remains supersonic almost until the flow enters the diffuser, where pressure is restored by reducing the speed.

To illustrate the picture of changes in a number of parameters along the axis of outflows of currents, current lines are shown along the axis and changes in the Pressure (Figure 28) and velocity of flows (Figure 29).

Figure B-4. Pressure Distribution in the Ejector

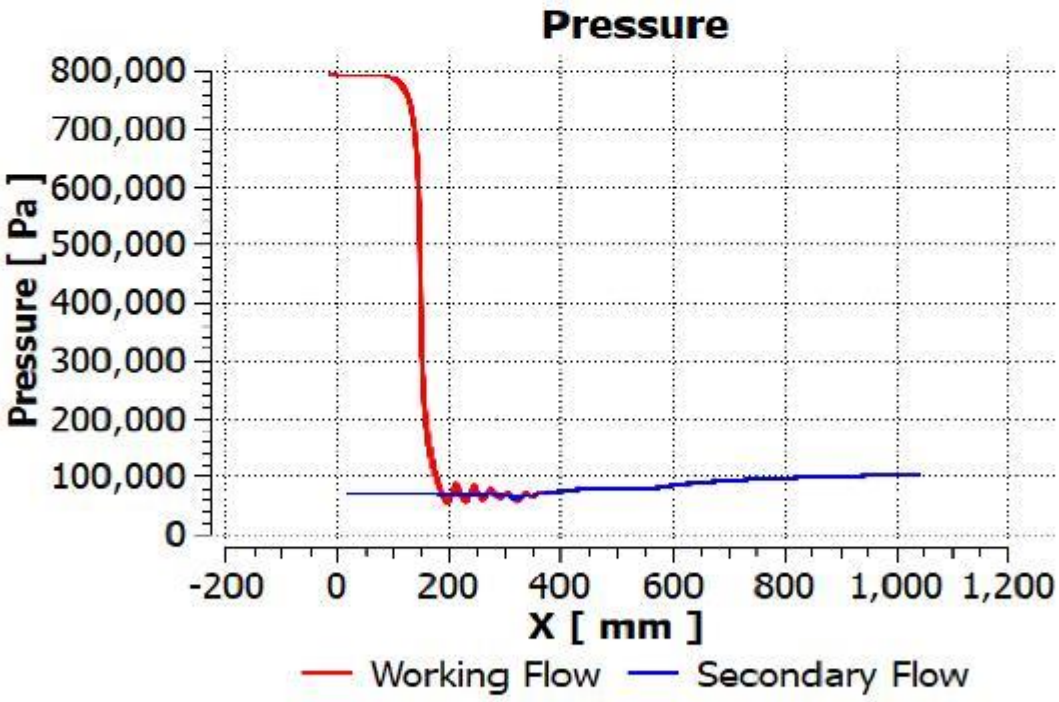

Cecil. Wilson Engineering

Figure B-5. Velocity Distribution in the Ejector

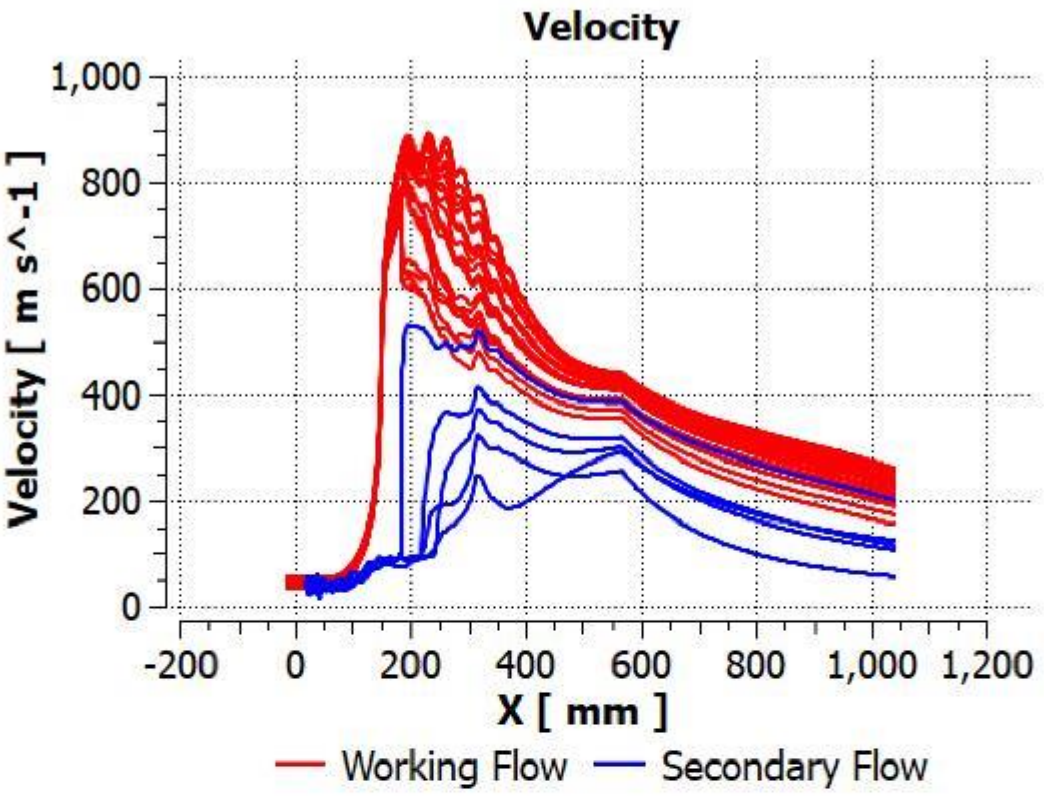

Credit: Wilson Engineering

APPENDIX C:
Photo Gallery

The sequence of key aspects of the project is captured here in photographs.

Martin Feed Site Visits

February 17, 2015 – Original Site Visit

December 16, 2015 – Second Site Visit

June 5, 2018 – Installation

The CEC site visit was held on June 5, 2018 when installation was nearly completed.

The project team on the host site during the CEC visit on June 5, 2018

August 30, 2018 – Commissioning and SCAQMD Compliance Testing

Commissioning of the demonstration unit was performed in late August of 2018.

UCNG natural gas supply equipment setting

Chimney with sampling lines

Natural gas and water supply connected to the demonstration unit

The ejector-system was stream pressurized and thermally insulated

Dynamic vacuum air locks for product discharge

Startup with steam venting


Preparation for startup and shakedown

September 6, 2018 – Feed Source Testing and System Shakedown Test 1


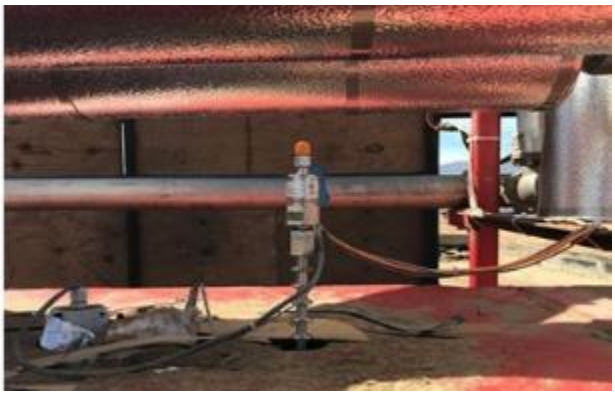

Control monitor and pressure sensor


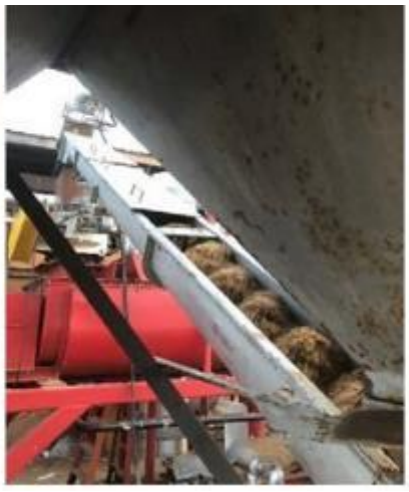


Product charging and discharging

Selected Equipment Photos

Prater Rotary Airlock Model PAV-1824 SS

Gear box and FVD motor for Holo-Flite.

Return Condensate Filter Feeding auger

APPENDIX D:
Control System Summary Report

SPURT, INC.

4033 Dana Court Northbrook, IL 60062

SUMMARY REPORT

GTI Project No.PIR-14-001/ Task 7/8.

Installation at the Martin-Feed facility for Indirect Gas-Fired Dryer with Advanced Heat Pump for Bulk Food Processing.

1. Task 7.1 Sensors' specification, control system startup and operating settings.

The control operating electrical package consisting of stand-alone single door stainless steel NEMA 4X enclosure and a separate operator interface stainless steel box housing the graphical human-machine interface (HMI) terminal and main operating push buttons and power ON pilot light.

The electrical package controls were built per Electrical Schematics attached (Appendix 1). The sensor and actuator devices were specified by the P&ID diagram (Page 2) and also by the Sensors and Valve Excel spreadsheet (Appendix 2).

The major electrical components included in the system control were:

- Allen-Bradley MicroLogix1400 PLC (programmable logic controller);
- Maple System graphical interface terminal HMI5097NXL;
- Mean-Well 24VDC, 20A power supply;
- ABB Motor protector devices MS116;
- ABB Variable Frequency Drives ACS150 and ACS355;
- Step down control transformer 480/120VAC;
- Phoenix Ethernet switch;
- Circuit branch protection devices (fuses);
- Miscellaneous parts and materials.

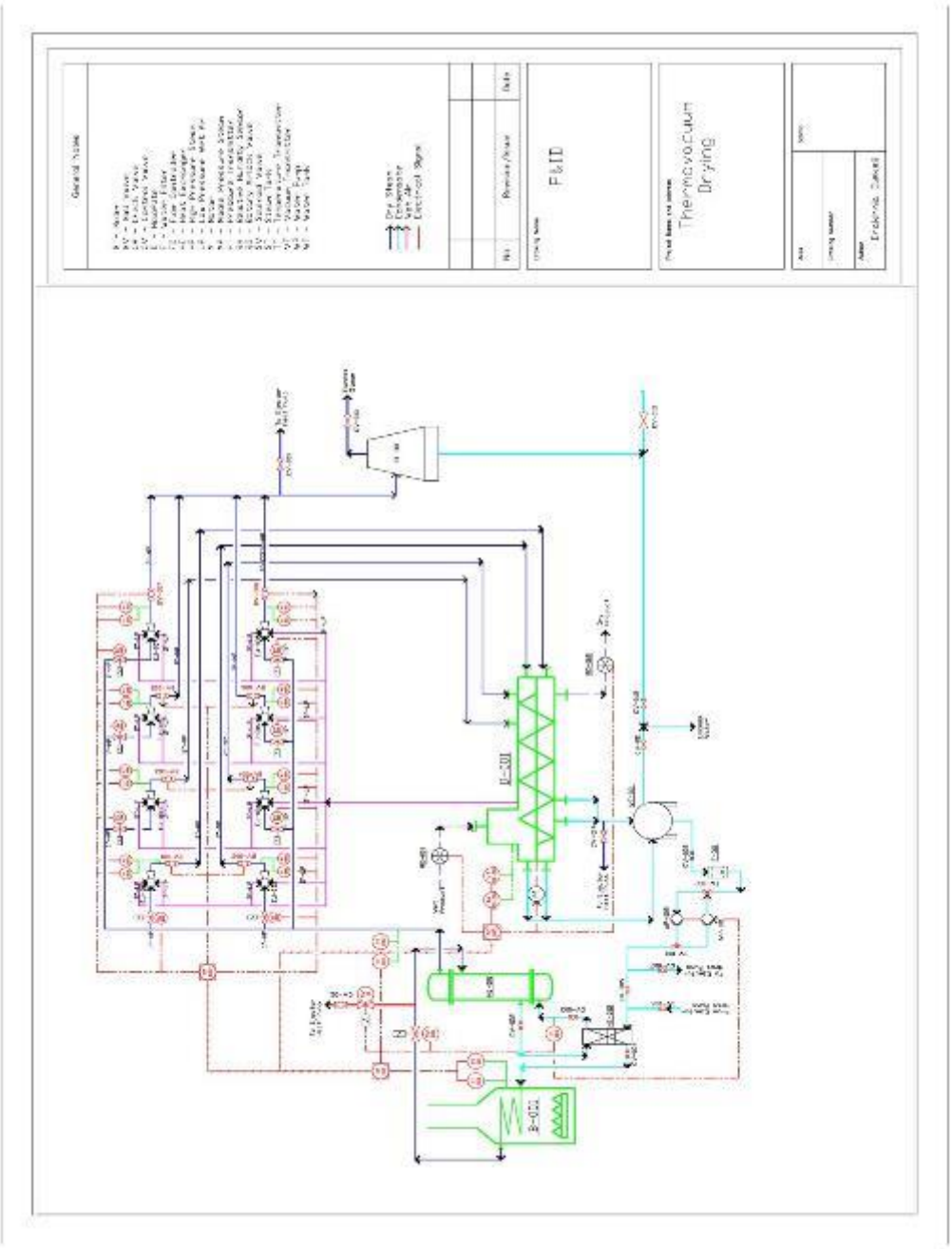

4033 Dana Court Northbrook, IL 60062

P&ID diagram

2. Task 7.2. Control system design adjustments and shakedown support.

During several business trips in the period from August to November 2018 the operating programming software was downloaded to the control system including programmable logic controller (PLC) and HMI and the system was commissioned for operation.

To connect all field instrumentation the control system utilized PLC expansion cards

- MicroLogix 1762 IT4 (thermocouple 4 point input card);
- MicroLogix 1762 IF4 (analog 4 point input card);
- MicroLogix 1762 OF4 (analog 4 point output card);
- MicroLogix 1762 OW16 (relay 16 point discrete output card).

Figure 1. Electrical Control Panel

3. Task 8.1 Measurement signals verification, debugging and sensors on-site calibration

All thermocouple (temperature) sensors were setup to J-type thermocouple input and verified by reference to the hand-held infrared pyrometer device.

All pressure transducer devices were setup to 4-20mA analog signal and calibrated per the reference specification.

All discrete (ON-OFF) actuator valves were tested by using on-device reference label flags. All analog (modulating proportional) actuator valves were tested and tuned by referencing to the on-device built-in status indicator (CLOSE-25%-50%-75%-OPEN).

Further in the testing process the pressure transducers were referenced to the manual pressure gauges installed at the same location.

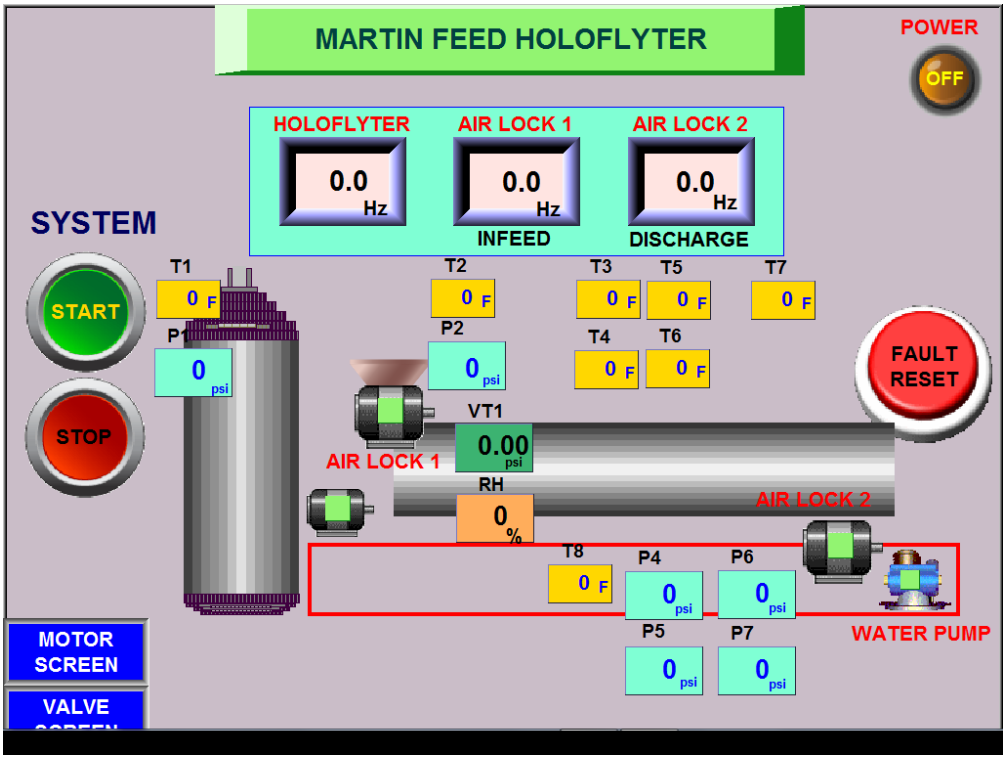

Figure 2. Operator HMI / Main Screen

The thermocouple sensors on the screen above (Figure 2) are labeled as T1 - T8 (process temperature). The pressure transducers on the screen above are labeled as P1-P2, P4 – P7 (pressure sensors). The other sensors are RH (relative humidity), VT1 (vacuum transducer), and not shown PH1, PH2 (product humidity).

4. Task 8.2 Control system operation manual for personnel training

The control system operation performed by the qualified personnel is provided from the Operator HMI mounted on the machine side (Fig. 3 below).

Figure 3. Operator HMI terminal.

When the system is ready to operate the machine should be powered by a mobile power generator providing electrical power 480VAC, 60A.

An operator should make sure the red E-Stop button is pulled out, press the green power ON button and the green pilot light get illuminated. On the Main Screen (Figure 2) the Power indicator in the upper right corner turns red flashing ON sign. The rest of the operations are performed from the Main Screen.

An operator should make sure that no alarm messages are displayed and reset them pressing on the red FAULT RESET button.

Press green SYSTEM START button at the upper left corner to start the system. All motors will start rotating at the speed ranging from 10 to 75 Hz displayed in the blue frames in the middle of the screen. These motors are Holoflyter, Air Lock 1, Air Lock 2 and fixed speed water pump. The speeds can be changed by touching each blue rectangular frame. The numeric keypad will pop-up, an operator can enter reference in Hz and press Enter button. When motor are running the green square indicators on each motor icon will start blinking.

The discrete solenoid valves operate from the Solenoid Valve screen (Figure 4).

To open/close each solenoid valve SOL 1-4 touch green rectangular ON/OFF button. When valve open the green square indicator light turns on. To open/close each ball valve BV 5-7 use individual OPEN and CLOSE rectangular buttons in each valve panel.

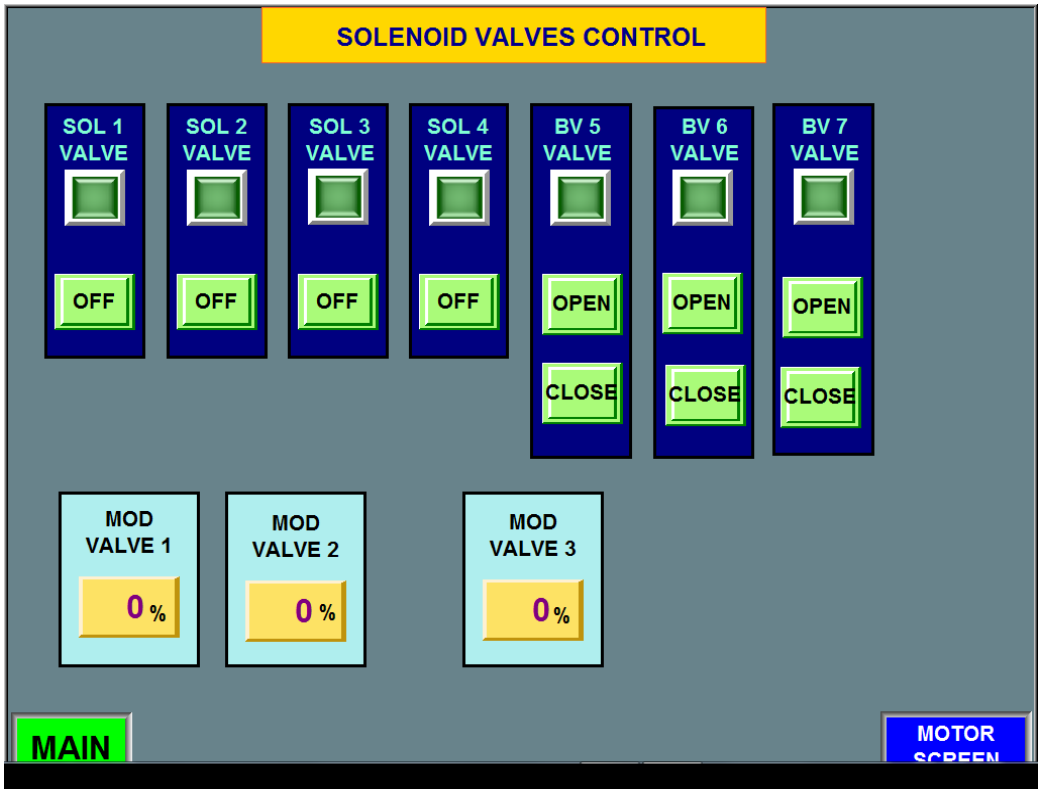

Figure 4. Solenoid Valves control screen.

The modulating proportional valves operate from the same screen. To control their operation an operator should press on the yellow rectangular frame. The numeric keypad will pop-up, an operator can enter desired percentage from 0 to 100% and press Enter button. The execution of those proportional valves can be observed on-device built-in status indicator (CLOSE-25%-50%-75%-OPEN).

To control and adjust each individual motor's operation for the maintenance purpose an operator should change the screen by pressing MOTOR SCREEN button on any other screens. That screen (Figure 5) allows to Start/Stop and adjust speed reference of Holoflyter and Air Lock 1 and 2 motors, as well as Start/Stop fixed speed Water Pump.

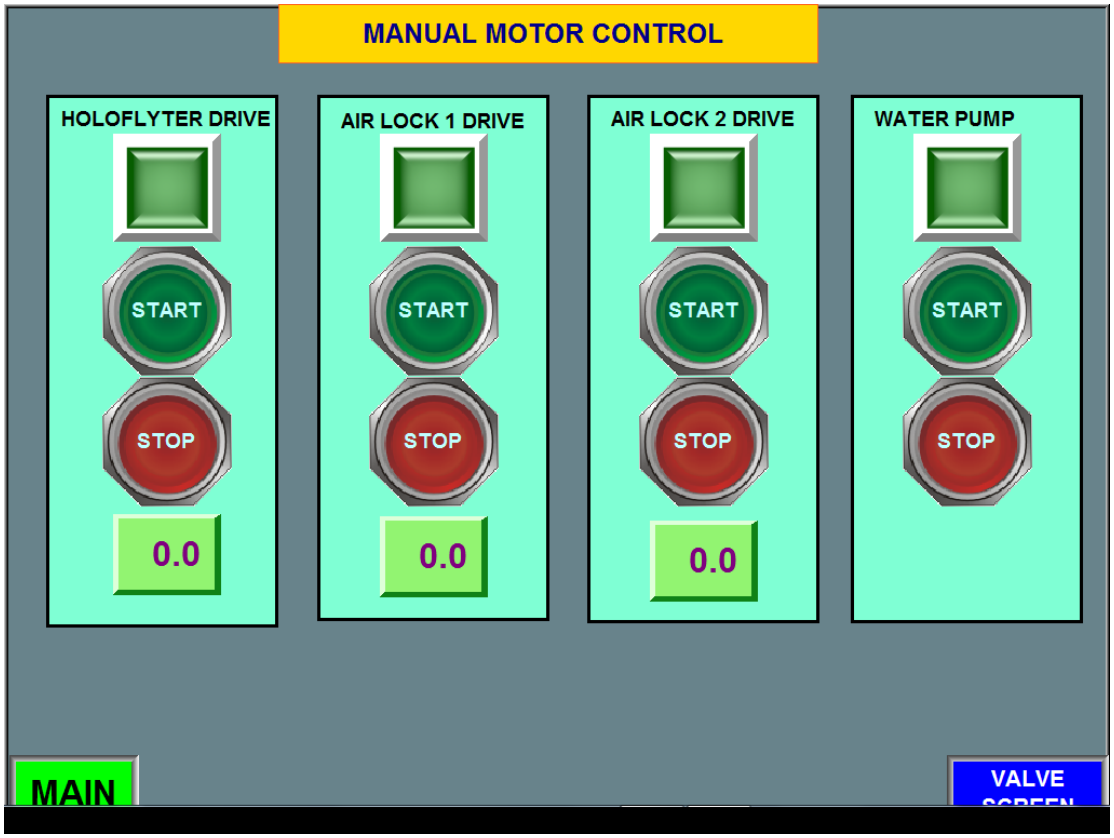

Figure 5. Manual motor control screen.

5. Task 8.3 Technical communications, reviews, and summary reporting

Provided technical communications with Wilson Engineering operating and maintenance staff and GTI engineers for the job specification, execution and follow up procedures.

Attachments:

Appendix 1. Gas-Fired Dryer Electrical Schematics.
Appendix 2. Sensors and Valves specification.

Signed by:

Mark Polin Spurt,
Inc. President,
MSEE